Title
THE EFFECT OF SILICON ON THE ENVIRONMENTAL CRACKING BEHAVIOR OF A HIGH STRENGTH STEEL

Author
Cedeno, M.H.C.

Publication Date
1977-05-01

LBL-6012
c.1

THE EFFECT OF SILICON ON THE ENVIRONMENTAL CRACKING BEHAVIOR OF A HIGH STRENGTH STEEL

Mario Herminio Castro Cedeño
(M. S. thesis)

May 1977

Prepared for the U. S. Energy Research and Development Administration under Contract W-7405-ENG-48

LAWRENCE BERKELEY LABORATORY
UNIVERSITY OF CALIFORNIA
BERKELEY

THE EFFECT OF SILICON ON THE ENVIRONMENTAL
CRACKING BEHAVIOR OF A HIGH STRENGTH STEEL

Contents

THE EFFECT OF SILICON ON THE ENVIRONMENTAL CRACKING BEHAVIOR OF A HIGH STRENGTH STEEL

Mario Herminio Castro Cedẽno

Materials and Molecular Research Division,
Lawrence Berkeley Laboratory and
Department of Materials Science and Engineering,
University of California, Berkeley, California 94720

ABSTRACT

The effect of silicon on the environmental cracking behavior of high strength steels was investigated by testing AISI 4340 and 300-M steels in various environments. Results show that whether it was used as an austenite stabilizer or as a solid solution strengthener, silicon reduced steady-state crack velocities by substantial amounts. Lifetimes, however, appear to depend more on fracture toughness than on any other parameter. The present work has confirmed that the environmental cracking behavior of a material can be modified by composition and heat treatment variation; therefore, the possibility of designing environmental cracking resistant alloys should be explored further.

I. INTRODUCTION

The addition of small quantities of silicon to steel above the amount needed for deoxidation is an accepted metallurgical practice. Some of the reasons for its use are that silicon is known to be a very potent solid solution strengthener of iron and also because it increases the hardenability of steel[1-4]. Silicon also retards the softening of steel on tempering, thus permitting higher tempering temperatures to be used without severe loss of tensile strength[4-7]. Also, the ability of silicon to stabilize the austenite phase[1,4] could become another incentive for its use as an alloying element, since retained austenite is believed to increase the fracture toughness of high strength steels[8-13].

Another interesting result of adding silicon to steel is an enhancement of the corrosion resistance. Investigators[14,15] have reported improved general corrosion resistance commonly attributed to the formation of a silica (SiO_2) film which protects the material from further corrosion. The existence of this film is generally accepted in silicon iron alloys and silicon cast irons. Glazkova[16] reported a reduction of pitting corrosion in a silicon modified austenitic stainless steel. Stress corrosion cracking resistance can also be improved by means of silicon additions. Lees, et. al.[17] propose the use of silicon to increase the repassivation rate, i.e. to accelerate the formation of a protective film and in this way increase the resistance to stress corrosion cracking. Carter[18,19] reported a reduction in the subcritical flaw growth rate for a silicon modified 4340 steel tested in distilled water when compared to the original alloy.

It was silicon's desirable and sometimes unexpected enhancement of the corrosion resistance of steels which was of interest in this work. Specifically, the effect of silicon on the environmental cracking behavior of high strength steels was investigated from two points of view: when silicon was used as a strengthener and when used as an austenite stabilizer.

Previous work on the effect of silicon on the environmental cracking of high strength steels include that of Carter[18,19], in which 4340 steel with various amounts of silicon ranging between 0.09 to 2.15 percent was tested. His results showed that at a high tensile strength level (280 to 300 Ksi) silicon additions cause no marked change in the threshold stress intensity (K_{ISCC}), but resulted in a significant reduction in the crack growth rate. At low tensile strength levels (230 to 240 Ksi) no difference in the crack growth rate was noted for various amounts of silicon. The mechanism for this behavior was not completely elucidated but it was proposed that silicon containing epsilon carbides somehow retarded the process. Gerberich[20,21] attributes the enhanced cracking resistance to reduced lattice diffusivity of hydrogen.

Little work has been conducted on the effect of retained austenite on the stress corrosion cracking resistance of steels. One of the few projects reported in the literature is that of Webster[22] who reported a direct correlation between the amount of retained austenite and the threshold stress intensity. In addition, McCoy and Gerberich[23], Dulis and Chandohk[24] and Gold and Koppenoal[25] have reported high resistance of austenitic steels to hydrogen embrittlement. These are encouraging results; the generally accepted mechanism of stress corrosion cracking of high strength steels proposes that hydrogen generated by cathodic reaction migrates to the region of maximum triaxial stress and there leads to hydrogen-assisted cracking[26-38].

II. MATERIALS PREPARATION AND EXPERIMENTAL METHODS

A. Materials Selection and Preparation

The alloys used in this investigation were aircraft quality AISI 4340 and 300-M. Table I shows typical chemical composition of the two alloys. The silicon content of the 300-M alloy is substantially higher than that of 4340. Bars three inches in diameter were forged, annealed and rough-machined into fracture toughness (K_{IC}) specimens and blanks for tensile test specimens (Fig. 1).

B. Heat Treatment

Austenitizing was carried out in a vertical tube furnace in an argon atmosphere for one hour. Specimens were quenched by opening the bottom of the furnace and dropping the bars into the quench medium. The specimens were then tempered for one hour in a salt bath.

For this investigation the quenching medium and the tempering temperature were varied. First, both 4340 and 300-M were heat treated according to commercial specifications (i.e. austenitizing at 870°C, oil quenched and tempered at 200°C for the 4340 and at 300°C for the 300-M). Next, a heat treatment was selected for the 300-M which produced a good combination of strength and toughness and a fairly large amount of retained austenite. This heat treatment consisted of austenitizing at 870°C, quenching and holding in brine at 250°C for one hour, followed by quenching to room temperature, and then tempering at 300°C (referred to hereafter as the isothermal heat treatment). Finally, two heat treatments were selected which produced the same yield strengths but virtually no retained austenite in both 300-M and 4340. The heat treatments were as follows: 300-M austenitized at 870°C, oil quenched and tempered at 470°C; and 4340 austenitized at 870°C, oil quenched and tempered at 300°C. With these heat treatments the effect of silicon on the cracking behavior was studied in the absence of austenite. To examine the effect of retained austenite, the 300-M tempered at 470°C was compared with 300-M isothermally transformed at 250°C. The five heat treatments and the resulting properties are shown in Table II.

C. Mechanical Testing

After heat treatment, mechanical test specimens were machined to the final dimensions shown in Figures 1a and 1b. For the Fracture toughness specimens this involved surfacr grinding 0.025 cm from each face in order to remove any decarburized layer and machining a notch for the clip-in displacement gauge (Fig. 2d). The specimens were then pre-fatigued in air at room temperature with 135,000 kg MTS machine between maximum and minimum loads of 800 kg and 130 kg respectively, until total crack size of 0.2035 cm was reached. The fracture toughness tests, performed in the same machine, followed standard E-399-72 and were conducted at a machine crosshead of 0.10 cm/minute. The results are shown in Table II.

Tensile specimens were ground from previously heat treated blanks. The grinding and polishing was done under flood cooling to minimize heating of the test piece. The tensile tests were conducted at room temperature in the same MTS testing machine used for fracture toughness tests at a machine crosshead speed of 0.10 cm/min. The results are shown in Table II.

D. Environmental Cracking Tests

The specimens for the environmental cracking tests were prepared in a similar fashion to those used in the fracture toughness tests. After fatiguing they were tested in specially constructed machines (Figs. 2a and 2b). Specimens were attached to one end of a lever of the machine and submerged under water at room temperature. Distilled water, containing a 3.5 weight percent of sodium chloride, and deoxidized distilled water, obtained by bubbling nitrogen gas through distilled water, were used. At the other end, a load was fixed which remained constant during the test. A clip-in displacement gauge (Figs. 2c and 2d) was attached to the specimen and the amplified output was connected to a strip chart recorder running at constant speed. The gauge output was converted to crack length by means of a compliance calibration (Appendix B). With the aid of a computer program a crack growth rate versus stress intensity graph was obtained (Appendix C). Each of the crack growth rate versus stress intensity curves (Figs. 4 through 6) show the test points for two or more test specimens.

In addition lifetime curves were obtained (Fig. 3). This was done by recording the time-to-failure of the specimens. After the failure, the size of the original fatigue crack was measured as recommended in section 8.2.3 of Standard E 399-7240. This involved measuring to a 0.0025 cm precision the size of the crack at the center of the crack front and midway between the center and the edge on each side. The initial stress intensity (K_I) was then determined by using the formula[40]:

$$K_I = P/BW^{1/2} [29.6 (a/w)^{1/2} - 185.5 (a/w)^{3/2} + 655.7 (a/w)^{5/2}$$

$$- 1017.0 (a/w)^{7/2} + 638.9 (a/w)^{9/2}]$$

where:

P = load on specimen

B = thickness of specimen

W = width of specimen

a = original crack length

The threshold stress intensity (K_{ISCC}) was established by determining the load at which no failure occcurred in 100 hours[41]. The specimen was then loaded to fracture in the MTS machine described before and the fatigue crack size determined. The threshold stress intensity was then calculated.

E. X-Ray Analysis

In order to measure the amount of retained austenite resulting from each heat treatment, a Picker x-ray diffractometer was used. Samples were cut from broken K_{IC} specimens and repeatedly polished and etched in a solution of 100 milliliters of hydrogen peroxide (H_2O_2) plus 4 milliliters of hydrofluoric acid (HF) to obtain an underformed surface. Cu $K\alpha$ radiation was used and the amount of retained austenite was calculated with the formula[42-44]:

$$V_\gamma = \frac{(R\alpha/R\gamma)I\gamma}{I_\alpha + (R\alpha/R\gamma)I\gamma}$$

where:

I = integrated intensity

V_γ = volume percent of retained austenite

$$R = \frac{1}{v^2} \quad |F|^2 \, P \, \frac{1 + \cos^2 2\theta}{\sin^2\theta \cos\theta} \quad e^{-2M}$$

v = volume of unit cell

P = multiplicity factor

F = structure factor

θ = Bragg angle

e^{-2M} = temperature factor

The reflections used were the average of the (311) γ and (220) γ and (211) α. The limit of accuracy for this method is between 5-10%[43].

F. Metallography

1. Fractography

All fracture surfaces of the environmental cracking tests were examined using an AMR Scanning Electron Microscope operated at 20 Kv. The fracture surfaces were covered with acetate replicating tape before cutting them to an acceptable size for viewing. The tape was later dissolved in acetone.

2. Optical Metallography

Specimens for optical metallography were cut from broken fracture toughness specimens. They were prepared by wet grinding successively on 120, 240, 320, 400, and 600 grit papers and then polishing on a one micron diamond wheel lubricated with kerosene. Either 2% or 5% nital solution was used as etchant. Prior austenite grain size was measured by first etching with the following solution:

Hydrochloric acid	5 milliliters
Picric acid	4 grams
Methyl alcohol	100 milliliters

3. Transmission Electron Microscopy

In order to study the retained austenite distribution throughout the material, a Siemens IA electron microscope was used. The microscope was operated at 100 kv and at a magnification of 20,000X. Foils were prepared in the following manner:

a) 0.025 inch thick slices were cut from broken fracture toughness specimens. This was done on a flood cooled Dimet cutter to prevent heating.

b) The slices were chemically thinned to about 0.002 inch in a solution of about 100 drops of hydrofluoric acid in 500 milliliters of hydrogen peroxide. The solution was kept at constant temperature by surrounding it with an iced water bath.

c) 2.3 millimeters diameter disks were spark cut in a EDM machine.

d) These thin disks were finally electropolished in a twin jet electropolisher at room temperature using a chromicacetic acid of the following composition:

Chromium tri-oxide (CrO_3)	75 grams
Acetic acid (CH_3COOH)	400 milliliters
Distilled water	20 milliliters

To identify the carbides, specimens were prepared in the following fashion. First, heat treated samples were mechanically polished successively on 120, 240, 320, 400 and 600 grit papers. They were then etched with a 5% nital solution and carbon was evaporated onto the etched surface under vacuum. The resulting carbon film was cut into squares about 2mm on a side which was extracted by exposing the sample to steam for about 10 minutes and then submerging it under water so that the carbon floated to the surface. The carbon squares were then cleaned in acetone and extracted with microscope grids and dried.

III. RESULTS

A. Environmental Cracking Tests

Lifetime curves for the five heat treatments are shown in Figure 3. The resulting threshold stress intensity (K_{ISCC}) was the same (within an experimental error of $\pm$ 0.6 MPa$\sqrt{m}$ for all heat treatments of the same material. For 300-M it was about 18.4 MPa$\sqrt{m}$ whereas for 4340 it was about 16.6 MPa$\sqrt{m}$. This result was obtained despite the differences in fracture toughness. The results were in agreement with the crack growth rate versus instantaneous stress intensity curves (Figs. 4 and 5) since these show that at low stress intensities (close to K_{ISCC}) crack growth rates were similar for all heat treatments of the same material.

One conspicuous result was the marked increase in lifetimes obtained with the isothermal heat treatment. At high stress intensities (above 25 MPa$\sqrt{m}$) the time-to-failure were over two times longer than those of the next best heat treatment (300-M tempered at 470°C). The results were confirmed by Figure 5, which shows crack growth rate in region II (plateau velocity) to be considerably slower for the isothermal heat treatment.

Another interesting result was the fact that the lifetime curves (Fig. 3) of the two commercial heat treatments did not show any measurable difference. Their crack growth rate at a given stress intensity, however, is substantially different (Fig. 4). This apparent inconsistency was due to the fact that most of the lifetime of the part was spent in what is called the incubation period. During this period there is no crack growth and the chemistry of the solution changes from a neutral to an acidic nature[29]. The length of the incubation period varied from 50 per cent of the lifetime for specimens loaded to a low initial stress intensity to 90% of the lifetime for specimens loaded to high initial stress intensities. The lifetime, therefore, was dominated by the incubation period and large differences in propogation rates were required to make observable variations.

Another apparent inconsistency is the fact that 300-M tempered at 300°C and 470°C have similar crack velocities at the same stress intensity (Figs. 4 and 5), but different lifetimes (Fig. 3). This can be explained if it is noted that the fracture toughness of the long lifetime material is higher than that of the other. The results were not surprising since a higher fracture toughness means that, for a given load, the crack had to travel farther at very low velocities. An example will prove the point:

The stress intensity can be calculated with the formula:

$$K_I = P/BW^{\frac{1}{2}}\{f(a/w)\} \tag{2.1}$$

where:

K_I = Plane strain stress intensity

P = Load

B = Thickness of specimen

W = Width of specimen

$f(a/w)$ = A geometric factor depending on the variables w and a.

a = crack length

Since lifetime curves are determined mainly by fracture toughness of the material, another test is needed for elucidating the effect of silicon on the cracking resistance of the material. One possible way of doing this is by comparing their crack growth rate versus instantaneous stress intensity curves. These show three distinct regions commonly named I, II and III. Regions I and III show a very steep dependence of crack growth rate on stress intensity while region II is the flat part of the curve. All three regions can be explained by the environmental cracking model mentioned before[27,30]. At low stress intensities hydrogen migrates to the region of maximum tri-axial stress where it aids the fracture process, permitting the material to fracture at a lower stress intensity. Increasing stress intensities would reduce the hydrogen concentration needed to produce fracture, resulting in a faster crack growth rate. At high crack growth rates, however, the diffusion rate of hydrogen through the metal lattice is the limiting factor and the crack has to wait for the hydrogen to build up to the critical concentration. This results in region II where the crack growth is insensitive to the stress intensity. The crack velocity in region II is commonly referred to as the plateau velocity and since it depends on the diffusion rate of hydrogen through the lattice, it is a parameter which can be used to compare the effect of microstructure on the cracking resistance of a material. At stress intensities close to the fracture toughness of the material, the failure is mainly a mechanical process because the crack propagates so fast that hydrogen production and build-up cannot keep pace.

In Figure 6, when comparing materials of equal yield strength, the following was observed: First, that 300-M isothermally transformed had markedly reduced crack growth rates when compared to 300-M oil quenched and tempered at 470°C. This could be interpreted as meaning that retained austenite reduces the diffusion rate of hydrogen through the material and consequently increases environmental cracking resistance. Also the fact that 4340 oil quenched and tempered at 300°C had a higher crack growth rate than 300-M quenched and tempered at 470° may be considered as indication that increasing silicon content is beneficial to the cracking resistance of steels.

To further explore the effect of retained austenite on the environmental cracking of steels, tests wre conducted in a 3.5 weight-percent Sodium Chloride in distilled water solution. Since the mechanism for environmental cracking of austenitic steels is one in which the chloride ions act as catalysts for the anodic dissolution of austenite[39], an increased amount of austenite could be detrimental to the cracking resistance of the material. The two 300-M steel heat treatments of similar yield strength were tested and the results are shown in Figure 6. The resulting crack-growth-rate versus stress intensity curves are identical to the ones obtained with distilled water. Since the amount of retained austenite is less than ten percent, the results can most easily be explained if the environmental cracking mechanism working in the Sodium Chloride solution is the same mentioned before for tests in distilled water. Therefore, it can be stated with reasonable confidence that up to 10% retained austenite is a beneficial factor to the stress corrosion cracking resistance of high strength steels.

In order to elucidate the mechanism by which silicon in solution increases the resistance to environmental cracking of steels, various theories were tested. Hanna et, al.[33] reported that 300-M tested in deoxidized water had a shorter lifetime than similar material tested in regular distilled water. The result was explained in terms of oxide layer formation. Since the possibility existed of forming a protective layer of silica (SiO_2) as proposed by Lees, et. al.[17], it was decided to test 300-M in water which was deoxidized by bubbling nitrogen gas while conducting the test. If a silica film was being formed, testing in deoxidized water would stop its formation and consequently reduce lifetime and increase crack growth rate. The test was conducted and crack growth rate measured (Fig. 7). The results show that there was no significant change in crack propagation rate for 300-M tempered at 470°C and tested in distilled water and de-oxidized water. Carter[18] proposed that silicon containing epsilon carbides somehow enhanced the resistance to environmental cracking of steels. However, Figs. 4 and 5 show that the plateau velocity of 300-M steel tempered at 300°C is virtually similar to that of the same material tempered at 470°C. While carbides in the first case were epsilons carbides in the second case cementite (Fe_3C) was observed. In addition, Tinner and Gilping[53] attribute stress corrosion susceptibility of martensitic steels to the presence of epsilon carbides in the microstructure, however, this is a theory not generally held by other investigators[29]. Gerberich's argument of reduced diffusivity[20,21] is one mechanism that could account for the observed environmental cracking resistance of silicon containing steels. The fact that the effect is observed on the plateau velocity (diffusion dependent) and not on the threshold stress intensity is another factor in favor of Gerberich's theory. Supporting evidence is the work by Fletcher et. al.[54] in which silicon and chromium were found to decrease the diffusivity of hydrogen through steel.

B. Metallography

Figure 8 shows, for a single specimen, the effect of increasing stress intensity on the fracture surface. At low stress intensities (Fig. 8a and 8b, region II), the fracture surfaces were mainly intergranular with small amounts of tearing (arrows) and transgranular fracture (marked a). At high stress intensities (Fig. 8c, region III) a considerable amount of dimple rupture was also evident (marked b). Secondary cracks due to intergranular corrosion can be seen in all three surfaces.

Figure 9 shows, for a constant stress intensity, the effect of the heat treatment on the fracture surface. The fracture surfaces, all in region II, are predominantly intergranular with various amounts of tearing. Comparing the two commercial heat treatments (Figs. 9a and 9b) it can be seen that the 300-M shows a considerable amount of tearing. When comparing materials with equal yield (Figs. 9c through 9e), it can be seen that the material with the most tearing is the isothermal heat treatment whereas the least tearing was present in the 4340.

Final fracture surfaces are shown in Figure 10. Both commercial heat treatments (Figs. 10a and 10b) are similar with dimple rupture surfaces. The fracture surfaces of 4340 tempered at 300°C (Fig. 10c) and the 300-M tempered at 470°C (Fig. 10a) are both a combination of dimple rupture with some cleavage regions. The isothermal heat treatment, however, produced a completely different surface which can best be classified as quasi-cleavage.

Optical micrographs are shown in Fig. 11. Heat treatments a through d resulted in martensitic steels at various stages of tempering. However, the 4340 steel tempered at 200°C (Fig. 11a) shows little carbide precipitation during tempering. The isothermal heat treatment resulted in a lower bainitic structure with up to 50% martensite according to the TTT diagram[52].

Figure 12 is an electron micrograph of the 300-M steel isothermally heat treated. Figure 12a is the bright field and Fig. 12b is the dark field of the (002) austenite reflection. It is interesting to note that the austenite is between the martensite laths as observed by Lai[12] before. Since Shively et.al.[45] found the diffusivity of hydrogen through austenite is at least three orders of magnitude slower than through ferrite, it is possible that interlath austenite slows the diffusion of hydrogen through the material. This can be accomplished by either slowing the process or by limiting the hydrogen migration to the continuous martensite matrix, resulting in a longer path. Also, V.A. Kovalenko[46] reports that diffusion of hydrogen through bainite is considerably slower than through martensite (the time-temperature transformation diagram for

300-M shows that up to 50% bainite was formed with the isothermal heat treatment).

IV. DISCUSSION

A. Environmental Cracking Theories

Results of the present investigation are in agreement with the generally accepted mechanism explaining environmental cracking, the stress sorption[14,22] or decohesion[37,50] theories. These theories propose that hydrogen, either existing in the environment or produced by cathodic reaction in an aqueous environment, migrates to the regions of maximum triaxial stress where it aids the crack propagation process. The maximum diffusion rate at a given temperature results in a constant crack velocity over a wide range of stress intensities. This constant crack velocity, commonly called region II crack velocity, should depend on the diffusion rate of hydrogen through the lattice. The fact that silicon, retained austenite and lower bainite appear to work by reducing the diffusion rate of hydrogen through the lattice, is an encouraging sign.

The experiment, however, was not designed to refute the less popular internal pressure theory[29]. This theory proposes that hydrogen precipitates on internal voids and cracks, where it exerts a pressure on the surrounding material. This pressure is then believed to aid void coalescence and finally, fracture. The pressure theory, however, is most plausible for materials containing considerable amounts of hydrogen in solution at high temperatures which are then cooled to room temperature. Under such conditions a large hydrogen pressure is more likely to be produced on interval voids and cracks than from externally generated hydrogen. Also, the fracture surfaces observed were mostly intergranular with very little microvoid coalescence except at stress intensities close to the fracture toughness. It is very unlikely, then, that the internal pressure theory could explain the observed results as well as the stress sorption/decohesion theory.

Another theory which could account for the environmental cracking phenomenon is the purely electrochemical mechanism[51-53]. In this theory the stress aids the process by breaking any protective film that may form. However, in view of the fact that the existence of a silica (SiO_2) film was not confirmed and the good correlation observed between diffusion rates and region II crack velocities, it can be stated that the stress sorption/decohesion theory provides a better explanation of the observed facts.

B. Alloy Design

It has been shown that one of the main factors determining the lifetime of a part is the materials fracture toughness. Since a large amount of research has been devoted to that objective, it is possible to make use of that wealth of information in designing environmental cracking resistant alloys. The resulting alloys, promising to be of high fracture toughness and of high environmental cracking resistance, are bound to be technologically useful.

In addition to high fracture toughness, a low stage II crack growth rate is desired. Thic an be obtained by reducing the diffusion rate of hydrogen through the material. In the present experiment this was accomplished by the addition of silicon, the existence of retained austenite and by the presence of lower bainite on the structure. The optimization of these microstructural features, however, remains to be done.

V. CONCLUSIONS

From the available evidence the following statements can be made:

1. 1.6 per cent silicon in steel decreased the subcritical flaw growth rate by a substantial amount. The result was obtained when comparing materials of a similar yield strength and also when comparing materials of equal fracture toughness. Previous work[18] had shown this conclusion to be true for materials of similar ultimate tensile strength. The reduction in subcritical flaw growth rate was probably due to a reduction of the diffusivity of the hydrogen atoms.

2. A microstructure containing up to 10% retained austenite in the form of films between martensite/bainite laths showed considerably slower subcritical flaw growth rate when compared with quenched and tempered material of the same yield strength where virtually no austenite was present. The improvement was probably due to a slowing of the diffusion rate of hydrogen through the material.

3. The fracture toughness was one of the principal factors determining the lifetime of a component.

4. The environmental cracking behavior of a material can be modified through composition and heat treatment variations. Consequently, the possibility of optimizing the design of alloys resistant to environmental cracking should be explored further.

ACKNOWLEDGEMENTS

The author gratefully acknowledges the constant encouragement and guidance given in the course of this investigation by Professors E.R. Parker and V.F. Zackay. He would also like to express his gratitidue to Dr. R.O. Ritchie for suggesting the topic and for helping in every possible way.

The author is also thankful to Professor I. Finnie and G. Thomas for their valuable comments and to the entire technical support staff of the Materials and Molecular Research Division for their continuous help. Last, but not least, the author is thankful to his wife for her patience.

This work was done under the auspices of the U.S. Energy Research and Development Administration.

APPENDIX

A. Crack Growth Rate vs. Instantaneous Stress Intensity Curves

The first step in obtaining the crack growth rate versus instantaneous stress intensity curves was to analyze the raw data from the dead load tests. This data consisted of the output of the clip-in displacement gauge as recorded by a strip chart recorder moving at a constant speed (see Fig. 2d).

The output of the displacement gauges was in millivolts, but by a simple calibration procedure was converted into displacement. A compliance calibration, (see Section B, Appendix) permitted the calculation of crack size from the displacement information. Since the recorder was moving at constant speed, the time between displacement readings was known. Using both variables (crack size and time), the crack growth rate was calculated with the following formula:

A.1
$$\left.\frac{da}{dt}\right|_i = \frac{a_{i+1} - a_{i-1}}{2(\Delta t)}$$

where:

$\left.\frac{da}{dt}\right|_i$: Crack growth rate at time i.

a_{i+1} : Crack size at time i + 1.

a_{i-1} : Crack size at time i - 1.

Δt : Time between displacement readings.

The crack size was also used to calculate the stress intensity by means of the equation below:

$$\text{A.2} \qquad K_{Ii} = P/BW^{1/2} \left[29.6\,(a_i/w)^{1/2} - 185.5\,(a_i/w)^{3/2} + 655.7\,(a_i/w)^{5/2} - 1017.0\,(a_i/w)^{7/2} + 638.9\,(a_i/w)^{9/2}\right]$$

where:

K_{Ii} : Stress intensity at time i.

P : Load on specimen.

B : Thickness of specimen.

W : Width of specimen.

a_i : Crack length at time i.

All the previous calculations were programmed into a digital computer (section C, Appendix), whose output was the crack growth rate and the stress intensity as a function of elapsed time for all the specimens tested. The specimens were then divided into groups depending on their heat treatment and environment used for the test. Each one of the resulting curves (Figs. 4 through 7), contains the results of at least two different tests.

B. Compliance Calibration

The objective of the compliance calibration was to permit the calculation of the crack size (a) when the following was known: The load on the specimen (P), the specimen geometry (B,W), the clip-in gauge displacement (v) and Young's modulus (E).

The resulting equation was of the form:

$$\text{(A.3)} \qquad \frac{EBv}{P} = f\left(\frac{a}{w}\right)$$

To find the exact equation, a CTS specimen was used for calibration according to the following procedure: First, a crack of known size was made with 1/32 inch abrasive wheel. Next, the specimen was loaded in an MTS tensile test machine and a clip-in displacement gauge was attached. The load versus gauge reading (P vs. v) was obtained, and the slope dP/dv was measured. The left hand part of equation A.3 becomes:

$$\text{(A.4)} \qquad \frac{EBv}{P} = \frac{EB}{\frac{dP}{dv}}$$

This process was repeated for various crack sizes and plotted in semi-log graph paper with a/w on the arithmetic axis. Then, a power series fit to the data was obtained by using the least squares method (see page 137, reference 47). The resulting equation was:

$$\text{(A.5)} \qquad \mathrm{Log}_{10}\left(\frac{EBv}{P}\right) = 1.5129 - 1.0971\ (a/w) + 3.044\ (a/w)^2$$

However, what the computer program required was the crack size (a). In order to find a/w as a function of EBv/P, the following set of points were predicted with equation A.5.

a/w	log(EBv/P)
0.427	1.599
0.688	2.199
0.854	2.796

Next, the following equation was fitted through those data points:

$$a/w = a + b\,(\log EBv/P) + c(\log EBv/P)^2 \qquad \text{(A.6)}$$

This was done by solving the following three simultaneous equations:

$$0.427 = a + b(1.599) + c(1.599)^2$$
$$0.688 = a + b(2.199) + c(2.199)^2$$
$$0.854 = a + b(2.796) + c(2.796)^2$$

The solution was:

$a = -0.729$

$b = \ 0.9325$

$c = -0.131$

Figure 13 presents the plots of the original data and of equations A.5 and A.6.

C. Computer Program

Figure 14 shows the flow chart of the computer program while the print-out and results are shown below. As they are self-explanatory, no more comments are deemed necessary.

D. Identificaton of Carbides

Using a camera contant (λL) of 21.91 Åmm, the following lines were identified:

300-M TEMPERED AT 470°C

r(mm)	$d = \frac{\lambda L}{r}$	$(hk\ell)_{Fe_3C}$
6.4	3.42	
8.5	2.58	020
9.4	2.33	112,021
10.75	2.04	022 or 210
12.35	1.77	212
13.05	1.60	221
14.025	1.56	130

300-M TEMPERED AT 300°C

r	$d = \frac{\lambda L}{r}$	$(nkL)_{\varepsilon\text{-}Fe_2C}$
8.1	2.7	
9.38	2.34	100
10.3	2.13	002
12.08	1.81	
13.68	1.60	102
14.38	1.52	
19.5	1.12	112,201

```
000000B          PROGRAM STRESS(INPUT,OUTPUT,TAPE6)
001467B          DIMENSION V(100),T(100),A(100),CPR(100),CPC(100)
001467B          REAL K(100),K2(100)
           C
           C
           C
           C
           C
           C  INPUT DATA
           C
001467B          READ,E,B,W
           C         E=YOUNG'S MODULUS IN PSI
           C         B=THICKNESS IN INCHES
           C         W=WIDTH IN INCHES
           C
002771B       10 READ,P,N1,DT1,N2,DT2,ID,IHT
           C         P=LOAD IN POUNDS
           C         ID=IDENTIFICATION NUMBER (EG. M23)
           C         N1=NUMBER OF DATA POINTS (INITIAL PORTION OF DATA)
           C         N2=NUMBER OF DATA POINTS (FINAL PORTION OF DATA)
           C         DT1=TIME INTERVAL BETWEEN DATA POINTS (BEGINNING) IN HRS
           C         DT2=TIME INTERVAL BETWEEN DATA POINTS (END) IN HRS
           C         IHT=HEAT TREATMENT
           C          IHT=1-300M,A 870 C, OQ, T 300 C, DIST WATER
           C               2-300M,A 870 C, OQ T 470 C, DIST WATER
           C               3-300M,A 870 C, HOLD 250 C, OQ, T 300 C, DIST WATER
           C               4-300M,A 870 C, OQ T 470 C, NACL SOLN
           C               5-300M,A 870 C, HOLD 250 C, OQ, T 300 C, NACL SOLN
           C               6-4340,A 870 C, OQ, T 200 C, DIST WATER
           C               7-4340,A 870 C, OQ, T 300 C, DIST WATER
           C               8-4340,A 870 C, OQ, T 300 C, DEOXIDIZED WATER
           C
           C
           C
           C
           C
           C
003003B          N12=N1+N2
003004B          IF (P.EQ.0.0)GO TO 1000
003006B          WRITE (6,87)
003013B       87 FORMAT (1H1)
003013B          IF (IHT.GT.5)GO TO 25
003014B          WRITE (6,76)P,ID,IHT
003024B       76 FORMAT (53X,2HP=,F8.2,4H LBS,10X,4HID=M,I2,10X,4HIHT=,I1,//)
003024B          GO TO 26
003024B       25 WRITE (6,77)P,ID,IHT
003034B       77 FORMAT (40X,2HP=,F8.2,4H LBS,10X,3HID=,I2,10X,4HIHT=,I1,//)
003034B       26 WRITE (6,71)
003040B       71 FORMAT (15X,4HTIME,10X,12HCRACK LENGTH,16X,16HSTRESS INTENSITY,12X
                1,17HCRACK GROWTH RATE)
003040B          WRITE (6,72)
003044B       72 FORMAT (15X,5H(HRS),11X,8H(INCHES),12X,8H(KSI IN),8X,7H(MPA M),16X
                1,7H(IN/HR),8X,9H(MIC/SEC))
003044B          T0=0.0
           C
           C
           C        INPUT COD DATA (V(I)) IN INCHES
           C
```

```
                C
0030448               DO 81 I=1,N12
0030478               READ,V(I)
                C
0030558               ALG=ALOG 10(E*B*V(I)/P)
0030638               AW=(0.9325*ALG)-0.729-(0.131*(ALG**2))
0030708               A(I)=AW*W
0030718               K(I)=(P/(8*SQRT(W)))*((29.6*(AW**.5))-(185.5*(AW**1.5))+(655.7*(AW
                     1**2.5))-(1017.*(AW**3.5))+(638.9*(AW**4.5)))*.001
0031308               K2(I)=K(I)*1.099
0031318               T(I)=TO
0031338               IF (I.LT.N1)GO TO 91
0031358               GO TO 92
0031368            91 TO=T(I)+DT1
0031418               GO TO 81
0031428            92 TO=T(I)+DT2
0031448            81 CONTINUE
0031478               IF (N1.EQ.1)GO TO 94
0031518               DO 82 J=2,N1-1
0031548               CPR(J)=(A(J+1)-A(J-1))/(2.*DT1)
0031578            82 CPC(J)=CPR(J)*2.54*2.77778
0031638               IF (N2.EQ.0)GO TO 94
0031648               DO 84 J=N1+1,N12-1
0031708               CPR(J)=(A(J+1)-A(J-1))/(2.*DT2)
0031738            84 CPC(J)=CPR(J)*2.54*2.77778
0031778            94 WRITE (6,73)T(1),A(1),K(1),K2(1)
0032108            73 FORMAT (13X,F8.4,10X,F7.4,14X,F6.2,9X,F6.2)
0032108               IF (N1.EQ.1)GO TO 23
0032118               DO 83 L=2,N1-1
0032158            83 WRITE (6,74)T(L),A(L),K(L),K2(L),CPR(L),CPC(L)
0032408            74 FORMAT (13X,F8.4,10X,F7.4,14X,F6.2,9X,F6.2,15X,F8.4,9X,F8.4)
0032408               IF (N2.EQ.0)GO TO 99
0032418               IF (N2.EQ.1)GO TO 98
0032438               DO 86 L=N1+1,N12-1
0032478            86 WRITE (6,74)T(L),A(L),K(L),K2(L),CPR(L),CPC(L)
0032728               GO TO 99
0032738         98    WRITE(6,74)A(N1),K(N1),K2(N1),CPR(N1),CPC(N1)
0033118            99 WRITE (6,73)T(N12),A(N12),K(N12),K2(N12)
0033258            23 GO TO 10
0033258          1000 STOP
0033308               END
```

P= 1878.00 LBS ID=M30 IHT=3

CRACK LENGTH (INCHES)	STRESS INTENSITY (KSI IN)	(MPA M)	CRACK GROWTH RATE (IN/HR)	(MIC/SEC)
.8699	21.84	24.01		
.8777	22.07	24.26	.0116	.0819
.8815	22.19	24.39	.0095	.0669
.8872	22.36	24.58	.0075	.0531
.8891	22.42	24.64	.0165	.1161
.9037	22.88	25.14	.0181	.1280
.9072	22.99	25.27	.0105	.0744
.9142	23.22	25.51	.0272	.1917
.9344	23.89	26.25	.0330	.2327
.9472	24.33	26.74	.0190	.1343
.9534	24.56	26.99	.0242	.1710
.9714	25.22	27.71	.0267	.1881
.9801	25.55	28.08	.0280	.1975
.9994	26.31	28.92	.0350	.2473
1.0151	26.96	29.63	.0319	.2250
1.0313	27.67	30.41	.0339	.2391
1.0490	28.48	31.30	.0409	.2887
1.0722	29.61	32.54	.0487	.3438
1.0977	30.95	34.02	.0544	.3839
1.1266	32.62	35.85	.0632	.4459
1.1609	34.83	38.27	.0656	.4630
1.1923	37.08	40.76	.0632	.4462
1.2242	39.67	43.59	.0715	.5042
1.2637	43.31	47.60	.0700	.4940
1.2942	46.50	51.11	.0597	.4216
1.3235	49.93	54.87	.0672	.4743
1.3614	54.95	60.39	.0664	.4684
1.3899	59.20	65.06	.0581	.4101
1.4195	64.12	70.47	.0591	.4168
1.4489	69.55	76.43	.0571	.4032
1.4767	75.21	82.65	.0531	.3745
1.5020	80.88	88.89		

P= 1724.70 LBS ID=M53 IHT=5

CRACK LENGTH (INCHES)	STRESS INTENSITY (KSI IN)	STRESS INTENSITY (MPA M)	CRACK GROWTH RATE (IN/HR)	CRACK GROWTH RATE (MIC/SEC)
.8338	19.12	21.01		
.8698	20.06	22.04	.0284	.2004
.8906	20.63	22.68	.0383	.2701
.9464	22.32	24.53	.0576	.4066
1.0059	24.41	26.82	.0608	.4293
1.1056	28.83	31.68	.0690	.4870
1.1371	30.55	33.58	.0682	.4813
1.1739	32.81	36.06	.0721	.5089
1.2093	35.28	38.78	.0654	.4616
1.2393	37.65	41.37	.0523	.3689
1.2615	39.58	43.49	.0607	.4282
1.3000	43.30	47.58	.0681	.4804
1.3296	46.56	51.16		

P= 1700.50 LBS ID=M56 IHT=4

CRACK LENGTH (INCHES)	STRESS INTENSITY (KSI IN)	STRESS INTENSITY (MPA M)	CRACK GROWTH RATE (IN/HR)	CRACK GROWTH RATE (MIC/SEC)
.8717	19.82	21.79		
.8717	19.82	21.79	0	0
.8717	19.82	21.79	0	0
.8717	19.82	21.79	0	0
.8717	19.82	21.79	0	0
.8717	19.82	21.79	0	0
.8717	19.82	21.79	0	0
.8717	19.82	21.79	.0403	.2844
.9970	23.74	26.08	.2821	1.9906
1.0087	24.17	26.56	.1563	1.1030
1.0282	24.93	27.40	.2151	1.5175
1.0517	25.90	28.47	.2029	1.4318
1.0688	26.66	29.29	.2648	1.8684
1.1047	28.38	31.19	.3767	2.6580
1.1442	30.53	33.55	.4272	3.0144
1.1901	33.43	36.74	.3855	2.7196
1.2213	35.69	39.22	.3747	2.6434
1.2650	39.33	43.23	.4363	3.0784
1.3085	43.58	47.90	.4843	3.4167
1.3619	49.82	54.75	.5468	3.8582
1.4179	57.80	63.52	.5957	4.2027
1.4810	68.95	75.78	.7388	5.2124
1.5656	88.27	97.00		

P= 1724.70 LBS ID=M58 IHT=4

CRACK LENGTH (INCHES)	STRESS INTENSITY (KSI IN)	STRESS INTENSITY (MPA M)	CRACK GROWTH RATE (IN/HR)	CRACK GROWTH RATE (MIC/SEC)
1.0462	26.03	28.61		
1.0728	27.22	29.91	.1785	1.2592
1.0819	27.65	30.38	.1435	1.0123
1.1015	28.62	31.45	.2094	1.4773
1.1238	29.80	32.75	.2061	1.4538
1.1427	30.87	33.93	.1833	1.2931
1.1604	31.95	35.11	.1723	1.2154
1.1771	33.03	36.29	.2223	1.5687
1.2049	34.96	38.42	.2781	1.9622
1.2327	37.11	40.79	.2164	1.5267
1.2482	38.40	42.20	.1905	1.3442
1.2708	40.43	44.43	.2792	1.9698
1.3040	43.72	48.05	.3511	2.4769
1.3411	47.91	52.65	.3929	2.7719
1.3826	53.33	58.61	.3002	2.1179
1.4011	56.02	61.57	.5180	3.6550
1.4862	70.97	77.99	.7782	5.4905
1.5567	87.19	95.82		

P= 2767.00 LBS   ID=M20   IHT=2

CRACK LENGTH (INCHES)	STRESS INTENSITY (KSI IN)	(MPA M)	CRACK GROWTH RATE (IN/HR)	(MIC/SEC)
1.1772	52.99	58.23		
1.1837	53.69	59.00	.5452	3.8465
1.1881	54.17	59.54	.5091	3.5917
1.1938	54.82	60.24	.6642	4.6865
1.2014	55.68	61.19	.6053	4.2707
1.2059	56.22	61.78	.5448	3.8439
1.2123	56.97	62.61	.7099	5.0085
1.2201	57.94	63.67	.6939	4.8959
1.2261	58.69	64.50	.6743	4.7574
1.2336	59.66	65.56	.7798	5.5018
1.2417	60.73	66.74	.7973	5.6254
1.2496	61.80	67.92		

P= 2338.00 LBS   ID=M16   IHT=2

CRACK LENGTH (INCHES)	STRESS INTENSITY (KSI IN)	(MPA M)	CRACK GROWTH RATE (IN/HR)	(MIC/SEC)
.8764	27.43	30.15		
.8764	27.43	30.15	0	0
.8764	27.43	30.15	0	0
.8764	27.43	30.15	0	0
.8764	27.43	30.15	0	0
.9061	28.58	31.41	.3844	2.7119
1.2607	53.55	58.85		

P= 2767.00 LBS   ID=M20   IHT=2

CRACK LENGTH (INCHES)	STRESS INTENSITY (KSI IN)	(MPA M)	CRACK GROWTH RATE (IN/HR)	(MIC/SEC)
.8644	31.94	35.10		
.8644	31.94	35.10	0	0
.8644	31.94	35.10	.0017	.0117
.8777	32.52	35.74	.0042	.0296
.8980	33.44	36.75	.0052	.0368
.9194	34.46	37.87	.0055	.0387
.9418	35.58	39.10	.0047	.0328
.9567	36.35	39.95	.0046	.0325
.9787	37.56	41.28	.0058	.0409
1.0030	[illegible]	42.84	.0063	.0443
1.0290	[illegible]	44.63	.0072	.0507
1.0635	42.98	47.24	.0119	.0839
1.0665	43.20	47.48	.0233	.1647
1.0752	43.85	48.19	.1027	.7248
1.1178	47.29	51.97	.1834	1.2939
1.1669	51.91	57.05	.2332	1.6457
1.2345	59.76	65.68	.3292	2.3227
1.3315	75.04	82.46		

P= 1743.00 LBS   ID=M17   IHT=3

CRACK LENGTH (INCHES)	STRESS INTENSITY (KSI IN)	(MPA M)	CRACK GROWTH RATE (IN/HR)	(MIC/SEC)
.8195	18.96	20.84		
.8610	20.03	22.01	.0746	.5261
.8941	20.95	23.03	.0598	.4218
.9207	21.75	23.90	.0479	.3380
.9420	22.42	24.64	.0380	.2685
.9588	22.97	25.25	.0327	.2309
.9748	23.52	25.85	.0371	.2617
.9959	24.29	26.69	.0269	.1899
1.0017	24.51	26.93	.0198	.1399
1.0157	25.05	27.53	.0275	.1940
1.0292	25.59	28.12	.0187	.1318
1.0344	25.81	28.36	.0129	.0910
1.0421	26.13	28.72	.0176	.1244
1.0520	26.56	29.19	.0124	.0874
1.0545	26.67	29.31	.0096	.0681
1.0617	26.99	29.67	.0119	.0841
1.0664	27.21	29.90	.0151	.1063
1.0767	27.69	30.43	.0115	.0810
1.0778	27.75	30.49		

P= 1598.50 LBS   ID=M 4   IHT=1

CRACK LENGTH (INCHES)	STRESS INTENSITY (KSI IN)	(MPA M)	CRACK GROWTH RATE (IN/HR)	(MIC/SEC)
.9421	20.56	22.60		
.9496	20.78	22.84	.0183	.1293
.9568	21.01	23.09	.0393	.2775
.9810	21.78	23.93	.0699	.4935
1.0128	22.87	25.13	.0860	.6069
1.0498	24.27	26.67	.0922	.6508
1.0866	25.83	28.39	.0974	.6872
1.1277	27.82	30.58	.1046	.7378
1.1702	30.19	33.18	.1117	.7883
1.2171	33.25	36.55	.1151	.8118
1.2623	36.74	40.38	.1236	.8722
1.3160	41.72	45.85	.1327	.9362
1.3684	47.62	52.34	.1410	.9946
1.4288	55.98	61.53	.1602	1.1303
1.4966	67.77	74.47		

P= 2500.00 LBS   ID=M 5   IHT=1

CRACK LENGTH (INCHES)	STRESS INTENSITY (KSI IN)	(MPA M)	CRACK GROWTH RATE (IN/HR)	(MIC/SEC)
.5521	20.13	22.13		
.5588	20.25	22.25	.1239	.8745
.5686	20.42	22.45	.1458	1.0289
.5782	20.60	22.64	.1656	1.1684
.5907	20.85	22.91	.1393	.9826
.5968	20.97	23.05	.1352	.9538
.6087	21.22	23.32	.3022	2.1324
.6371	21.85	24.02	.2938	2.0732
.6479	22.11	24.30	.1600	1.1290
.6584	22.36	24.58	.2676	1.8878
.6835	23.01	25.29	.2963	2.0903
.6979	23.39	25.71	.2452	1.7303
.7162	23.91	26.27	.3324	2.3455
.7422	24.67	27.11	.4869	3.4352
.7811	25.89	28.46	.4355	3.0725
.8003	26.53	29.16	.3254	2.2960
.8245	27.38	30.09	.4681	3.3028
.8627	28.79	31.65		

P= 4240.00 LBS   ID= 2   IHT=7

CRACK LENGTH (INCHES)	STRESS INTENSITY (KSI IN)	STRESS INTENSITY (MPA M)	CRACK GROWTH RATE (IN/HR)	CRACK GROWTH RATE (MIC/SEC)
.9816	46.70	51.32		
.9941	47.57	52.28	1.8711	13.2016
1.0003	48.01	52.76	1.8036	12.7254
1.0122	48.87	53.71	2.4823	17.5143
1.0251	49.84	54.78	2.1240	14.9862
1.0334	50.49	55.49	1.8454	13.0203
1.0435	51.30	56.37	2.3780	16.7784
1.0572	52.42	57.61	2.9796	21.0227
1.0733	53.81	59.14	2.9177	20.5862
1.0864	54.99	60.43	2.6669	18.8166
1.1000	56.27	61.84		

P= 1402.70 LBS   ID= 4   IHT=7

CRACK LENGTH (INCHES)	STRESS INTENSITY (KSI IN)	STRESS INTENSITY (MPA M)	CRACK GROWTH RATE (IN/HR)	CRACK GROWTH RATE (MIC/SEC)
.9666	15.12	16.62		
1.0589	17.39	19.11	.0095	.0670
1.1567	20.59	22.63	.0073	.0516
1.2053	22.62	24.85	.0039	.0274
1.2343	24.01	26.39		

P= 1450.00 LBS   ID=15   IHT=6

CRACK LENGTH (INCHES)	STRESS INTENSITY (KSI IN)	STRESS INTENSITY (MPA M)	CRACK GROWTH RATE (IN/HR)	CRACK GROWTH RATE (MIC/SEC)
.9370	14.99	16.47		
.9501	15.27	16.78	.0783	.5527
.9526	15.32	16.84	.1827	1.2893
.9866	16.09	17.68	.4063	2.8668
1.0339	17.28	18.99	.5936	4.1880
1.1053	19.42	21.34	.9960	7.0271
1.2331	24.75	27.21	1.3335	9.4083
1.3720	34.10	37.47	1.5931	11.2399
1.5517	55.56	61.06		

P= 1757.50 LBS   ID=14   IHT=6

CRACK LENGTH (INCHES)	STRESS INTENSITY (KSI IN)	STRESS INTENSITY (MPA M)	CRACK GROWTH RATE (IN/HR)	CRACK GROWTH RATE (MIC/SEC)
.9072	17.44	19.17		
.9190	17.72	19.48	.5606	3.9553
.9259	17.89	19.66	.3423	2.4155
.9304	18.00	19.78	.3258	2.3690
.9371	18.17	19.97	.3315	2.3389
.9415	18.28	20.09	.1964	1.3856
.9437	18.34	20.15	.1297	.9151
.9458	18.39	20.21	.1289	.9094
.9479	18.45	20.27	.1915	1.3514
.9522	18.56	20.40	.3773	2.6619
.9605	18.78	20.64	.6733	4.7503
.9746	19.16	21.06	.5995	4.2295
.9805	19.33	21.24	.2919	2.0595
.9844	19.44	21.36	.2302	1.6242
.9882	19.55	21.48	.2837	2.0017
.9938	19.71	21.66	.4452	3.1409
1.0030	19.98	21.96	.5444	3.8408
1.0120	20.25	22.26	.5298	3.7384
1.0207	20.52	22.55	.4656	3.2851
1.0275	20.74	22.79		

P= 1711.00 LBS ID=60 THT=8

CRACK LENGTH (INCHES)	STRESS INTENSITY (KSI IN)	(MPA M)	CRACK GROWTH RATE (IN/HR)	(MIC/SEC)
.8690	19.88	21.84		
.8796	20.16	22.16	.1050	.7408
.8900	20.45	22.48	.1507	1.0636
.9098	21.02	23.10	.1927	1.3594
.9285	21.58	23.72	.1737	1.2258
.9445	22.09	24.27	.1731	1.2210
.9631	22.69	24.94	.1732	1.2221
.9792	23.24	25.55	.2997	2.1144
1.0231	24.88	27.34	.3756	2.6500
1.0543	26.17	28.76	.3093	2.1822
1.0849	27.57	30.30	.3621	2.5548
1.1267	29.72	32.67	.4131	2.9149
1.1676	32.14	35.33	.4193	2.9583
1.2106	35.10	38.58	.5210	3.6761
1.2718	40.19	44.17	.6322	4.4603
1.3370	47.05	51.70	.7672	5.4131
1.4252	59.33	65.21		

P= 1711.00 LBS ID=61 THT=8

CRACK LENGTH (INCHES)	STRESS INTENSITY (KSI IN)	(MPA M)	CRACK GROWTH RATE (IN/HR)	(MIC/SEC)
.9117	21.08	23.16		
.9249	21.47	23.60	.0840	.5930
.9285	21.58	23.72	.0454	.3206
.9339	21.75	23.91	.0450	.3172
.9375	21.86	24.03	.0616	.4349
.9463	22.14	24.33	.0949	.6695
.9565	22.47	24.70	.0925	.6527
.9648	22.75	25.00	.1134	.8004
.9792	23.24	25.55	.1485	1.0480
.9945	23.79	26.15	.1496	1.0552
1.0091	24.33	26.74	.1768	1.2473
1.0298	25.15	27.64	.2011	1.4186
1.0493	25.96	28.53	.1890	1.3333
1.0676	26.77	29.42	.2059	1.4526
1.0905	27.84	30.60	.2408	1.6992
1.1158	29.13	32.02	.2479	1.7488
1.1401	30.48	33.49	.2545	1.7960
1.1667	32.09	35.27	.2896	2.0435
1.1980	34.19	37.57	.3405	2.4021
1.2348	36.98	40.64	.3973	2.8031
1.2774	40.73	44.76	.4662	3.2894
1.3280	46.00	50.56	.5621	3.9662
1.3899	53.93	59.27		

P= 1723.70 LBS ID=452 THT=5

CRACK LENGTH (INCHES)	STRESS INTENSITY (KSI IN)	(MPA M)	CRACK GROWTH RATE (IN/HR)	(MIC/SEC)
.8658	19.94	21.91		
.8658	19.94	21.91	0	0
.8658	19.94	21.91	0	0
.8658	19.94	21.91	0	0
.8658	19.94	21.91	.0105	.0742
.8868	20.51	22.55	.0280	.1974
.9466	22.32	24.53	.0575	.4060
.9793	23.42	25.74	.0623	.4398
1.0090	24.51	26.94	.0696	.4913
1.0489	26.13	28.72	.0731	.5159
1.0821	27.64	30.38	.0711	.5018
1.1200	29.58	32.51	.0698	.4924
1.1519	31.41	34.52	.0668	.4716
1.1869	33.67	37.00	.0689	.4859
1.2208	36.14	39.72	.0664	.4685
1.2533	38.82	42.66	.0647	.4566
1.2855	41.81	45.95	.0645	.4552
1.3178	45.19	49.66	.0609	.4294
1.3463	48.52	53.33	.0539	.3805
1.3717	51.80	56.93	.0523	.3689
1.3986	55.62	61.12		

P= 1711.00 LBS   ID=60   IHT=8

CRACK LENGTH (INCHES)	STRESS INTENSITY (KSI IN)	(MPA M)	CRACK GROWTH RATE (IN/HR)	(MIC/SEC)
.8690	19.88	21.84		
.8796	20.16	22.16	.1050	.7408
.8900	20.45	22.48	.1507	1.0636
.9098	21.02	23.10	.1927	1.3594
.9285	21.58	23.72	.1737	1.2258
.9445	22.09	24.27	.1731	1.2210
.9631	22.69	24.94	.1732	1.2221
.9792	23.24	25.55	.2997	2.1146
1.0231	24.88	27.34	.3756	2.6500
1.0543	26.17	28.76	.3093	2.1822
1.0849	27.57	30.30	.3621	2.5548
1.1267	29.72	32.67	.4131	2.9149
1.1676	32.14	35.33	.4193	2.9583
1.2106	35.10	38.58	.5210	3.6761
1.2718	40.19	44.17	.6322	4.4603
1.3370	47.05	51.70	.7672	5.4131
1.4252	59.33	65.21		

P= 1711.00 LBS   ID=61   IHT=8

CRACK LENGTH (INCHES)	STRESS INTENSITY (KSI IN)	(MPA M)	CRACK GROWTH RATE (IN/HR)	(MIC/SEC)
.9117	21.08	23.16		
.9249	21.47	23.60	.0849	.5930
.9285	21.58	23.72	.0454	.3206
.9339	21.75	23.91	.0450	.3172
.9375	21.86	24.03	.0616	.4349
.9463	22.14	24.33	.0949	.6695
.9565	22.47	24.70	.0925	.6527
.9648	22.75	25.00	.1134	.8004
.9792	23.24	25.55	.1485	1.0480
.9945	23.79	26.15	.1496	1.0552
1.0091	24.33	26.74	.1768	1.2473
1.0298	25.15	27.64	.2011	1.4186
1.0493	25.96	28.53	.1890	1.3333
1.0676	26.77	29.42	.2059	1.4526
1.0905	27.84	30.60	.2408	1.6992
1.1158	29.13	32.02	.2479	1.7488
1.1401	30.48	33.49	.2545	1.7960
1.1667	32.09	35.27	.2896	2.0435
1.1980	34.19	37.57	.3405	2.4021
1.2348	36.98	40.64	.3973	2.8031
1.2774	40.73	44.76	.4662	3.2894
1.3280	46.00	50.56	.5621	3.9662
1.3899	53.93	59.27		

P= 1723.70 LBS   ID=WR2   IHT=5

CRACK LENGTH (INCHES)	STRESS INTENSITY (KSI IN)	(MPA M)	CRACK GROWTH RATE (IN/HR)	(MIC/SEC)
.8658	19.94	21.91		
.8658	19.94	21.91	0	0
.8658	19.94	21.91	0	0
.8658	19.94	21.91	0	0
.8658	19.94	21.91	.0105	.0742
.8868	20.51	22.55	.0280	.1974
.9466	22.32	24.53	.0575	.4060
.9793	23.42	25.74	.0623	.4398
1.0090	24.51	26.94	.0696	.4913
1.0489	26.13	28.72	.0731	.5159
1.0821	27.64	30.38	.0711	.5018
1.1200	29.58	32.51	.0698	.4924
1.1519	31.41	34.52	.0668	.4716
1.1869	33.67	37.00	.0689	.4859
1.2208	36.14	39.72	.0664	.4685
1.2533	38.82	42.66	.0647	.4566
1.2855	41.81	45.95	.0645	.4552
1.3178	45.19	49.66	.0609	.4294
1.3463	48.52	53.33	.0539	.3805
1.3717	51.80	56.93	.0523	.3689
1.3986	55.62	61.12		

REFERENCES

1. E.C. Bain and H.W. Paxton, Alloying Elements in Steel, 5th ed. (American Society for Metals, Metals Park, Ohio, 1966)

2. M.A. Grossmann and E.C. Bain, Principles of Heat Treatment, 5th ed. (American Society for Metals, Metal Park, Ohio, 1964)

3. Republic Steel Corporation, Alloying Elements and their Effects, (Republic Steel Corp.,

4. C.H. Shih, B.L. Averbach and M. Cohen, Trans. of the ASM 48, 86 (1956)

5. C.J. Altstter, The Effect of Silicon on the Tempering of High Strength Steels, Sc.D Thesis, Massachusetts Institute of Technology, 1958

6. C.J. Altstter, Cohen and B.L. Averbach, Trans. of the ASM 55, 287 (1962)

7. A.A. Alten and P. Payson, Trans. of the ASM 45, 498 (1953)

8. J. McMahon and G. Thomas, Proceeding International Conference on Microstructure and Design of Alloys, Cambridge, Institute of Metals (London) 1, 180 (1973)

9. D. Webster, Trans. of the ASM 61, 816 (1968)

10. S.D. Antolovich, A. Saxena and G.R. Chamani, Met. Trans. 5, 623 (1974)

11. E.R. Parker, V.F. Zackay, G.Y. Lai and R.M. Horn, Untempered Ultra High Strength Steels of High Fracture Toughness, LBL-2715, Army Contract DAAG46-73-C-0120, April 1974.

12. G.Y. Lai, V.F. Zackay and E.R. Parker, Enhancement of Fracture Toughness by Retained Austenite in 300 M Steel, LBL-4513, Nov.1975

13. G.Y. Lai, W.E. Wood, R.A. Clark, V.F. Zackay and E.R. Parker, Met. Trans. 5, 1663 (1974)

14. H.H. Unlig, Corrosion and Corrosion Control, 2nd. ed., (John Wiley & Sons Inc., New York, 1971)

15. M.G. Fontana and N.D. Greene, Corrosion Engineering, (McGraw-Hill Book Co., New York, 1967)

16. S.A. Glazkova, L.I. Freiman, G.S. Raskin and G.L. Shvarts, Zashchita Metallov 6,660 (1972)

17. D.J. Lees, F.P. Ford and T.P. Hoar, Metals and Materials 7, 231 (1973)

18. C.S. Carter, The Effect of Silicon on the Stress Corrosion Resistance of Low-Alloy, High-Strength Steel, Advanced Research Projects Agency Contract N00014-66-Co265, March 1969.

19. C.S. Carter, Corrosion 25, 423 (1969).

20. W.W. Gerberich, Hydrogen in Metals, I.M. Bernstein and A.W. Thompson eds., American Society of Metals, Metals Park, Ohio, 1974

21. I.M. Bernstein and A.W. Thompson, International Metallurgical Reviews, in press December issue

22. D. Webster, the Stress Corrosion Resistance and Fatigue Crack Growth Rate of a High Strength Martensitic Stainless Steel, AFC 77, Boeing Document D6-23973, The Boeing Co., Seattle, Washington, June 1969.

23. R.A. McCoy and W.W. Gerberick, Met. Trans. 4, 539 (1973)

24. E.J. Dulis and V.K. Chendohk, Metals Progress 97, 101 (1969)

25. E. Gold and T.J. Koppenaal, ASM Trans. 62, 607 (1969)

26. A.H. Priest and P. McIntyre, Factors Influencing the Threshold Stress Intensity Values and Crack Propagation Rates During Stress Corrosion Cracking Tests of High Strength Steels, BISRA Report September 1971.

27. B.F. Brown, Stress-Corrosion Cracking in High Strength Steels and in Titanium and Aluminum Alloys, (U.S. Government Printing Office, Washington, D.C., 1972).

28. H.L. Logan, The Stress Corrosion of Metals, (John Wiley and Sons, Inc., New York, 1966).

29. R.W. Staehle, A.J. Forty and D. Van Roogen, Eds., Proceedings of Conference - Fundamental Aspects of Stress Corrosion Cracking, (NACE, Houston, 1969), References cited are in pages 407, 457 446 and 397.

30. H.P. Von Leeuwen, Corrosion 31, 42 (1975)

31. W.A. Van der Sluys, Mechanisms of Environment Induced Subcritical Flaw Growth Rate in AISI 4340 Steel, Theoretical and Applied Mechanics, University of Illinois, September 1966.

32. W.A. Van der Slys, Environmental Cracking in AISI 4340 Steel, Theoretical and Applied Mechanics Report No. 312, Dept. of Theoretical and Applied Mechanics, University of Illinois, February 1968.

33. G.L. Hanna, A.R. Troiano and E.A. Steigerwald, Trans of the ASM 57, 658 (1964)

34. C.D. Beachem, Met. Trans. 3, 437 (1972)

35. W.W. Gerberich and Y.T. Chen, Met. Trans. 64, 271 (1975)

36. E.G. Coleman, D. Weinstein and W. Rostoker, Acta Metallurgica 9, 491 (1961)

37. R.A. Oriani and P.H. Jospehic, Acta Metallurgica 22, 1065 (1974)

38. J.D. Landes and R.P. Wei, Int. Journal of Fracture 9, 277 (1973).

39. T.P. Hoar and J.C. Scully, Journal of the Electrochemical Society 11, 348 (1964).

40. Annual Book of ASTM Standards, (American Society for Testing of Materials, Philadelphia, 1972).

41. A.H. Priest and P. McIntire, Factors Influencing Threshold Stress Intensity and Crack Propagation Rates During Stress Corrosion Cracking of High Strength Steels, BISRA Report, September 1971.

42. R.L. Miller, Trans of the ASM 57, 892 (1964)

43. B.D. Cullity, Elements of X-ray Diffraction, (Addison-Wesley Publishing Co., Notre Dame, 1956).

44. J.S. Huang, Effects of Silicon Structures and Properties of AISI 4340 Low Alloy Steel (M.S. Thesis), LBL-4505, December 1975.

45. J.H. Shiveley, R.F. Hehemann and A.R. Troiano, Corrosion 22, 253 (1966).

46. V.A. Kovalenko, Soviet Materials Science 9, 353 (1973).

47. P.R. Bevington, Data Reduction and Error Analysis for Physical Sciences, (McGraw-Hill Publishing Co., New York, 1969).

48. R.A. Oriani and P.H. Josephic, Scripta Metallurgica 6, 681 (1972).

49. T.P. Hoar and J.C. Scully, Journal of the Electrochemical Society 111, 348 (1964)

50. Y. Katz in International Congress on Fracture:München, April 1973

51. G.P. Cherepanov in International Congress on Fracture: München, April 1973

52. C.E. Ericsson, An Isothermal Study of Bainitic and Martensitic Transformations in Some Low Alloy Steels Using a New Magnetic Permeability Technique (MS Thesis), LBL-2279, December 1973

53. N.A. Tiner and C.B. Gilpin, Corrosion 22, 271 (1966).

54. E.E. Fletcher, W.E. Berry and G.A. Elsea, DMIC Report No. 232 (1964) or see reference 29, p. 457.

TABLE I. CHEMICAL COMPOSITION OF ALLOYS INVESTIGATED

Alloys	Weight Percent										
	C	Mn	P	S	Si	Ni	Cr	Mo	Va	Cu	Fe
4340	0.41	0.8	0.006	0.004	0.26	1.75	0.79	0.23	None	.06	Balance
300-M	0.42	0.76	0.007	0.002	1.59	1.76	0.76	0.41	0.10		Balance

TABLE II. HEAT TREATMENTS AND THEIR PROPERTIES

Material	Heat Treatment	Prior Austenite Grain Size	% Retained Austenite		Sy	Su	K_{IC}	K_{ISCC}
		μm			MPa	MPa	$MPa\sqrt{m}$	$MPa\sqrt{m}$
4340	Austenitized at 870°C-Oil quenched Tempered at 200°C one hour	20	<2%		1652	2039		16.6
					1572	2135		
				Avg.	1612	2087		
4340	Austenitized at 870°C-Oil quenched Tempered at 300°C one hour	20	<2%		1476	1652	63.2	16.6
					1597	1842	60	
					1423	1770	65	
				Avg.	1498	1755	62.7	
300-M	Austenitized at 870°C Isothermal hold at 250°C for one hour-Oil quenched Tempered at 300°C one hour	20	10%		1425	1820	92.3	18.5
					1482	1832	87.4	
					1570	1934	85.7	
				Avg.	1492	1862	88.5	
300-M	Austenitized at 870°C-Oil quenched Tempered at 470°C one hour	20	<2%		1441	1701	67.2	18.0
					1526	1743	70	
					1523	1633	69.4	
				Avg.	1497	1683	68.9	
300-M	Austenitized at 870°C-Oil quenched Tempered at 300°C one hour	20	5%		1697	1940	67.2	18.6
					1728	2046	64.8	
					1787	2032	63.1	
				Avg.	1737	2006	65.1	

where: Sy: yield strength; Su: ultimate strength; K_{IC}: Plane strain fracture toughness; K_{ISCC}: Threshold stress intensity

FIGURE CAPTIONS

Fig. 1. Fracture toughness and tensile specimens used.

Fig. 2. Equipment used. (a) Creep machines and recorders. (b) Creep machines. (c) Environment container. (d) Clip-in displacement gauge and method of attachment.

Fig. 3. Lifetime curves for tests in distilled water.

Fig. 4. Crack propagation rate versus instantaneous stress intensity curves for commercial heat treatments (tests conducted in distilled water at room temperature).

Fig. 5 Crack propagation rate versus instantaneous stress intensity curves for equal yield strength heat treatments (tests conducted in distilled water at room temperature).

Fig. 6. Crack propagation rate versus instantaneous stress intensity curves for tests conducted in 3.5 weight percent sodium chloride solution.

Fig. 7. Crack propagation rate versus instantaneous stress intensity curves for tests conducted in deoxidation water.

Fig. 8. Effect of increasing stress intensity on fracture surface. Specimen was 4340 steel tempered at 300°C. (a) 30 $MPa\sqrt{m}$ (b) 40 $MPa\sqrt{m}$ (c) 50 $MPa\sqrt{m}$ (all stress intensities approximate).

Fig. 9. Effect of heat treatment on fracture surface. All surfaces formed at a stress intensity close to 35 $MPa\sqrt{m}$.
(a) 4340 tempered at 200°C (b) 300-M tempered at 300°C
(c) 4340 tempered at 300°C (d) 300-M tempered at 470°C
(e) 300M isothermally transformed.

Fig. 10. Final fracture surfaces. (a) 4340 tempered at 200°C (b) 300-M tempered at 300°C (c) 4340 tempered at 300°C (d) 300-M tempered at 470°C (e) 300M isothermally transformed

Fig. 11. Optical micrographs. (a) 4340 tempered at 200°C (b) 300-M tempered at 300°C (c) 4340 tempered at 300°C (d) 300-M tempered at 470°C (e) 300-M isothermally transformed. Etchant used was either 2 or 5 percent nital.

Fig. 12. Transmission electron micrograph of isothermally transformed 300-M showing retained austenite distribution. (a) Bright field. (b) Dark field. (c) Selected Area Diffraction Pattern. (d) Indexed Diffraction pattern.

Fig. 13. Plot of original data, compliance calibration and equation fitted to compliance calibration equation (See Appendix B for details).

Fig. 14. Flow chart of Computer program used to calculate crack propagation rate and stress intensities.

Fig. 15. Diffraction patterns obtained from carbon replicas. a) 300-M tempered at 300°C. b) 300-M tempered at 470°C. See Appendix D.

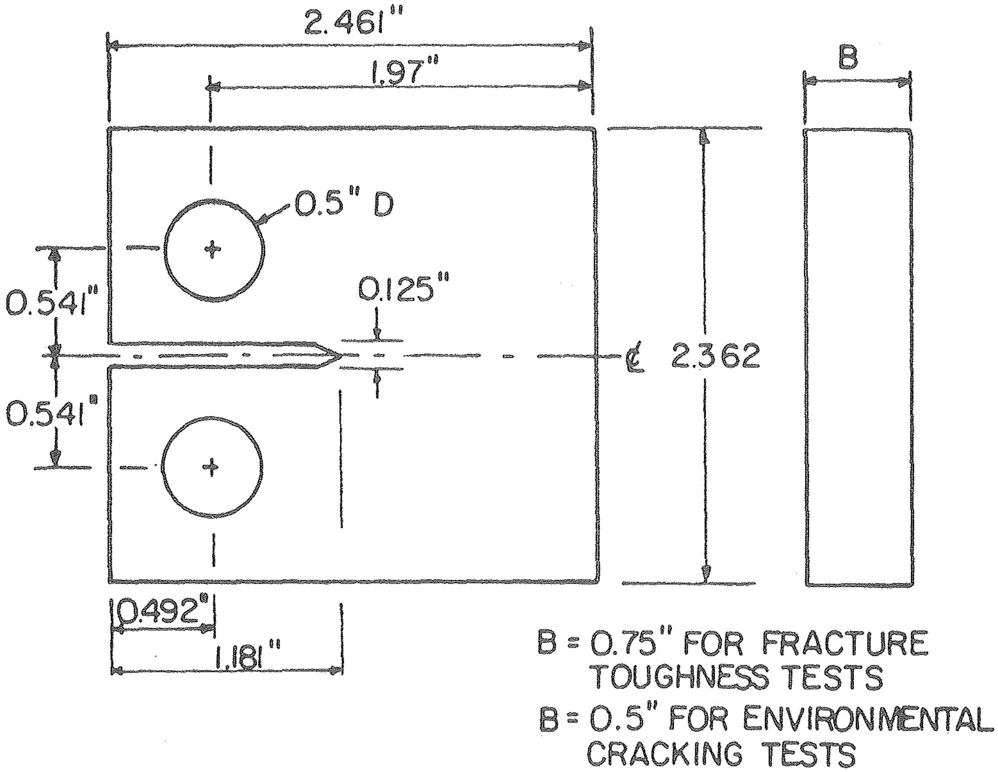

(a) FRACTURE TOUGHNESS SPECIMEN

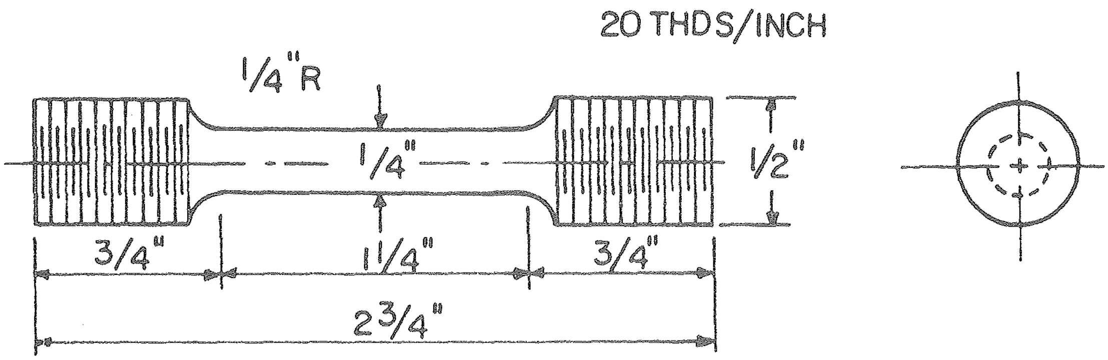

(b) ROUND TENSILE SPECIMEN

XBL 7611-7823

Fig. 1.

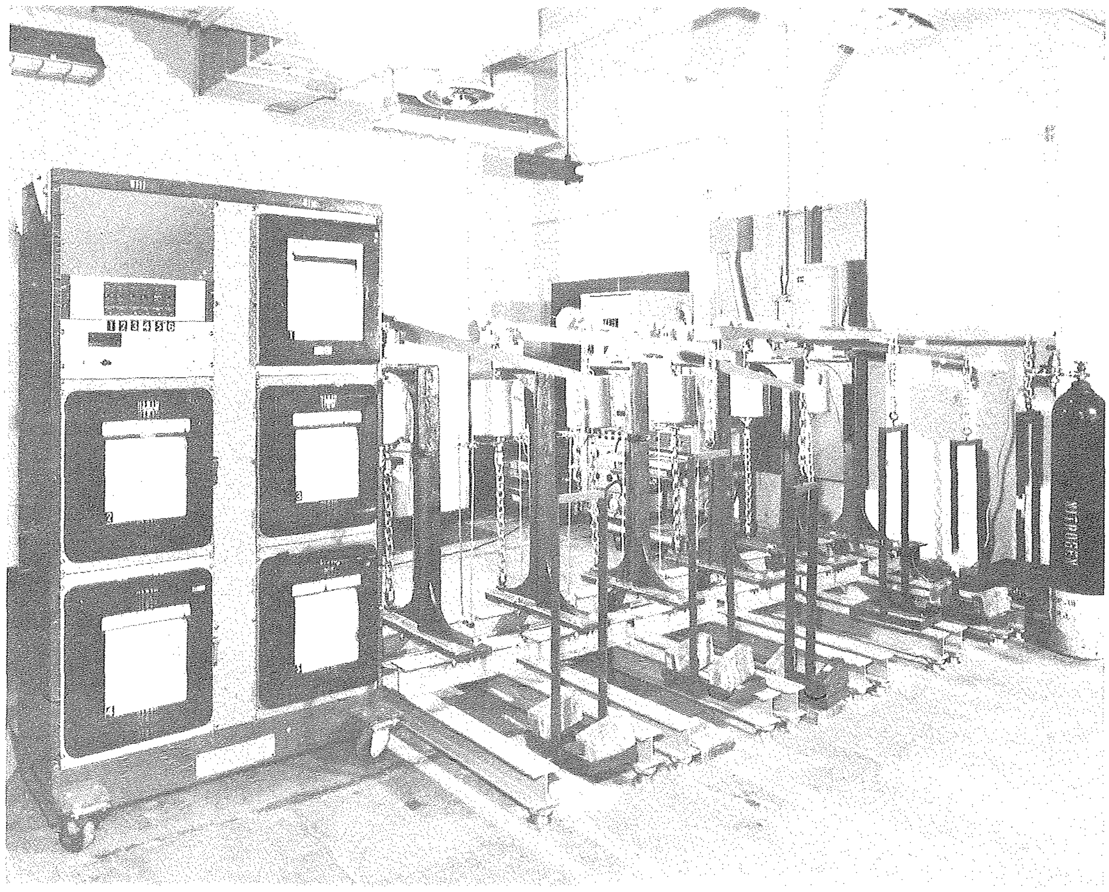

CBB 760-10246

Fig. 2a.

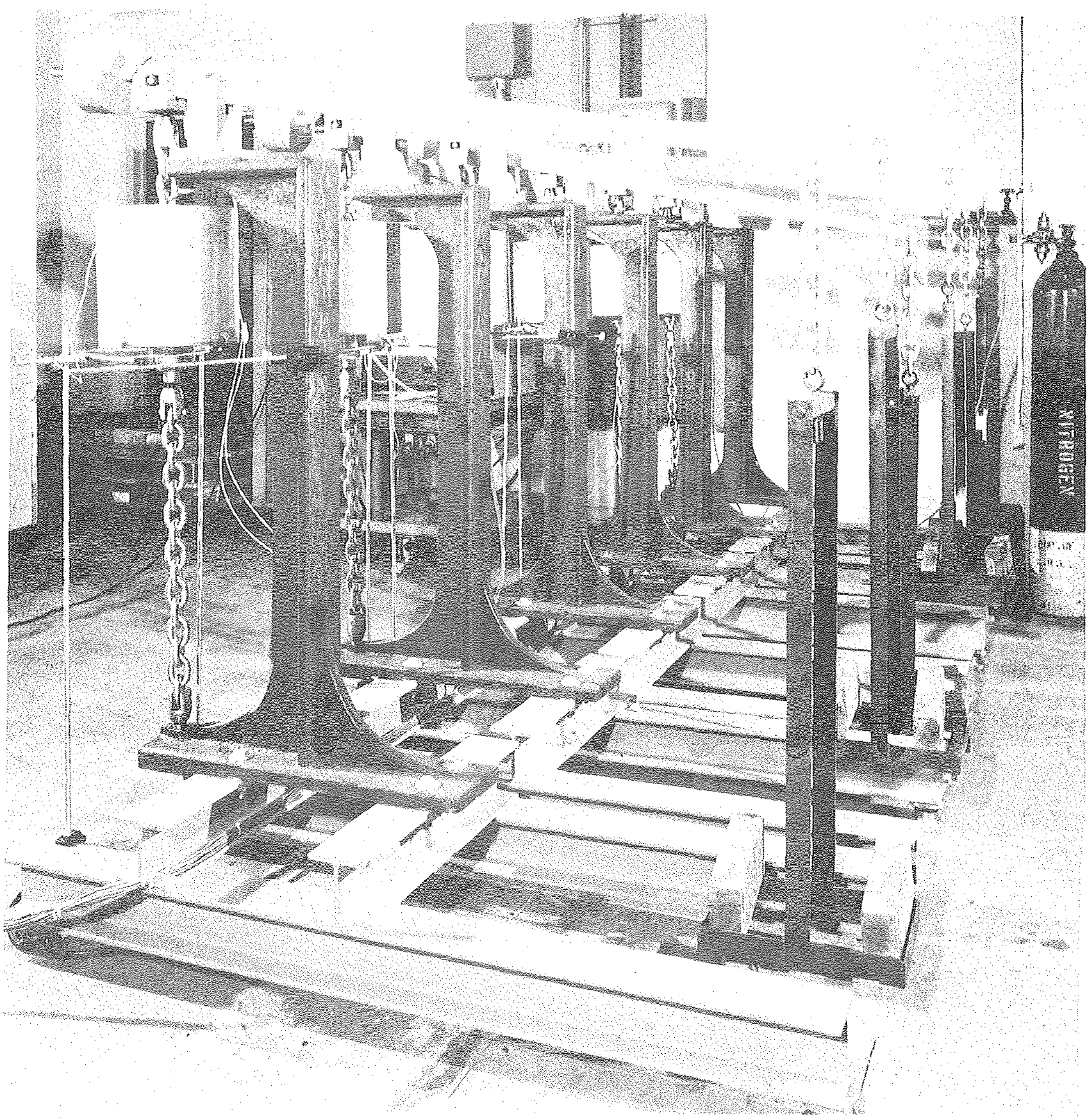

CBB 760-10248

Fig. 2b.

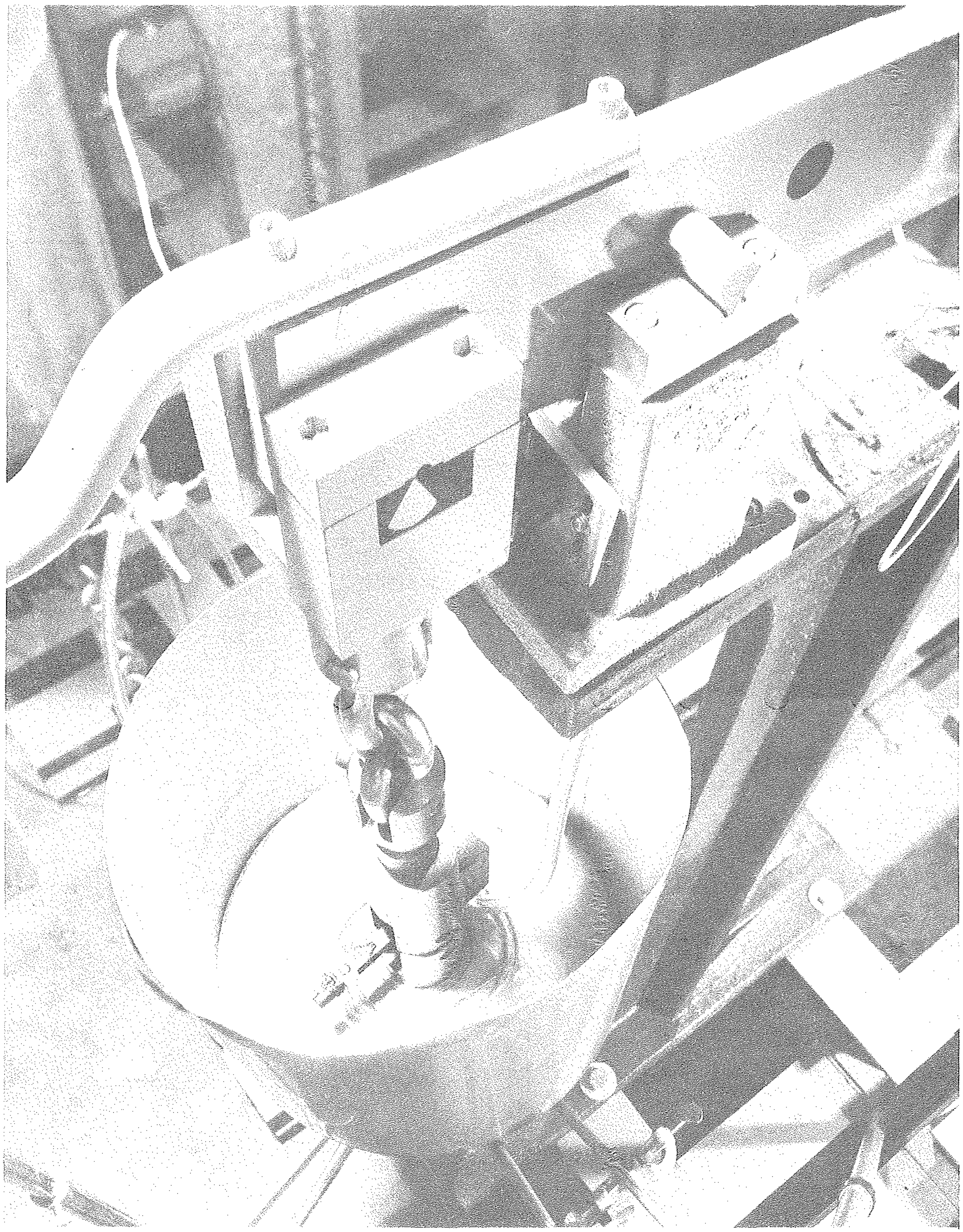

CBB 760-10244

Fig. 2c

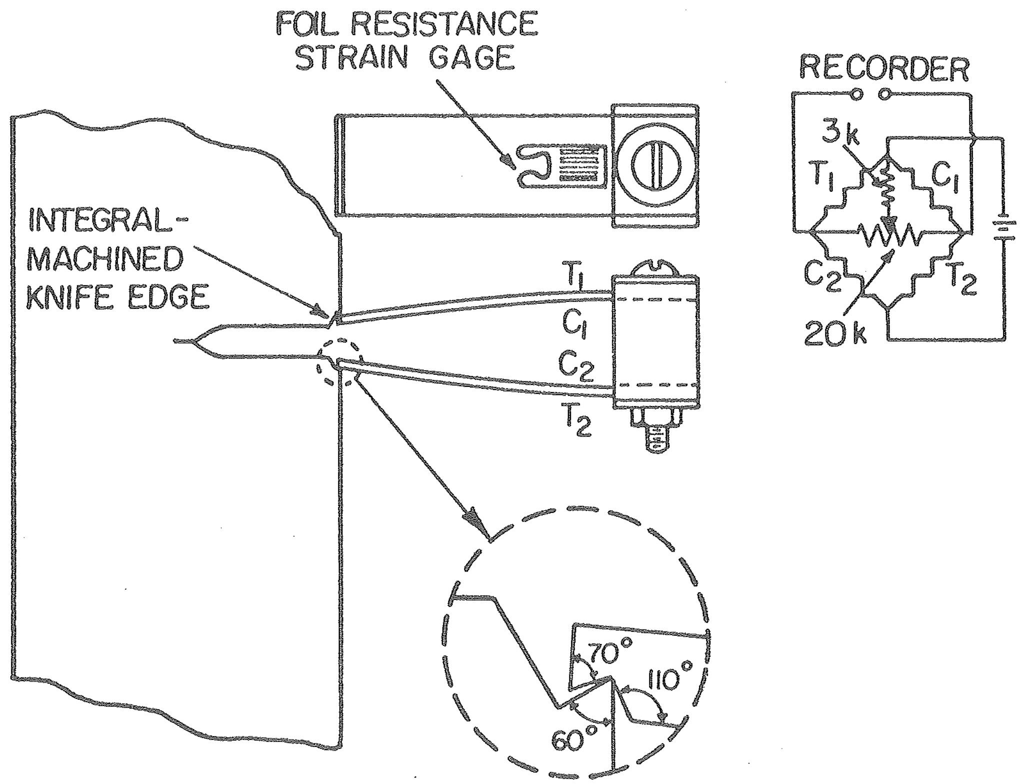

XBL 7611-7822

Fig. 2d

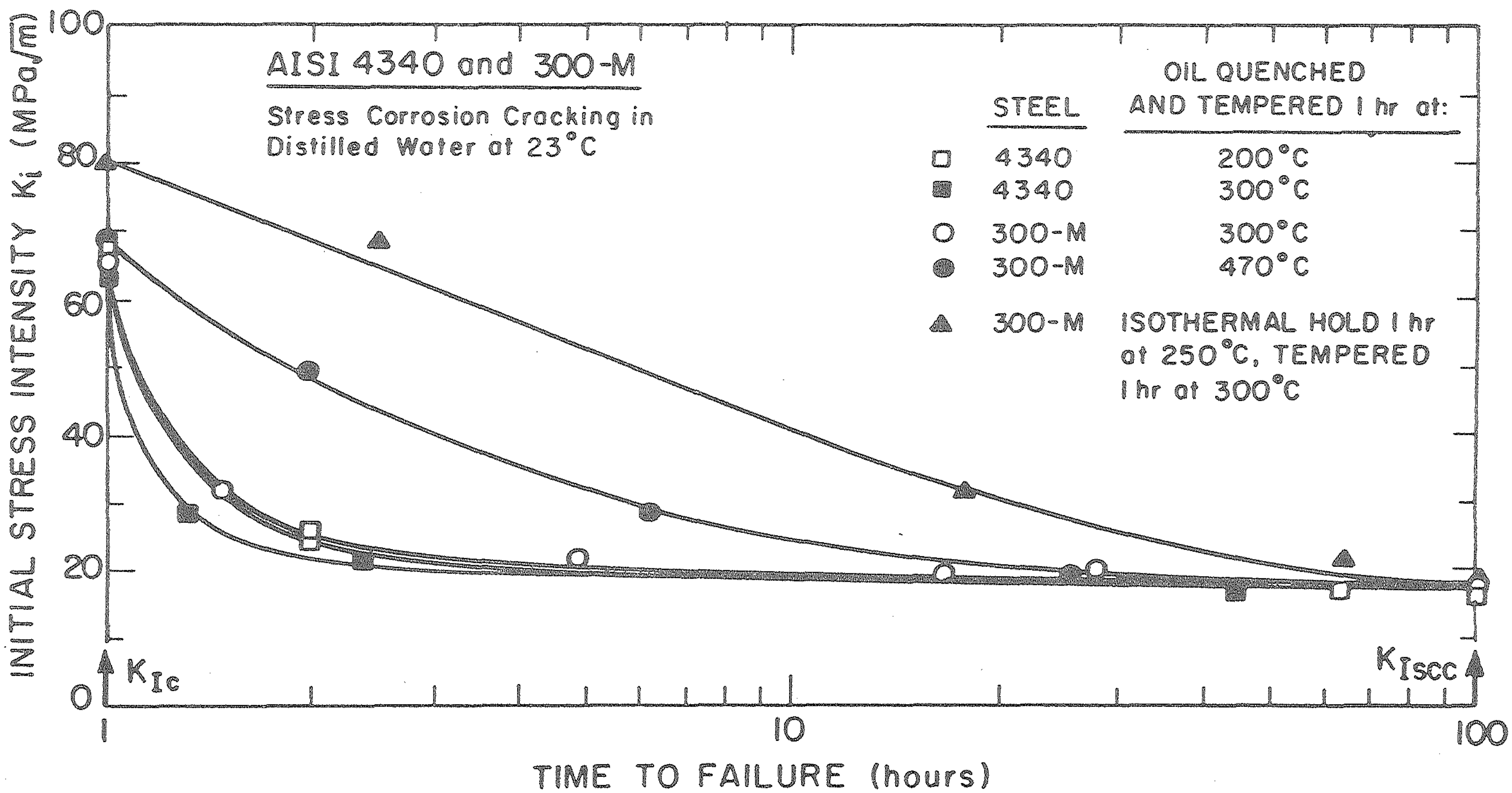

XBL 7610-7629

Fig. 3.

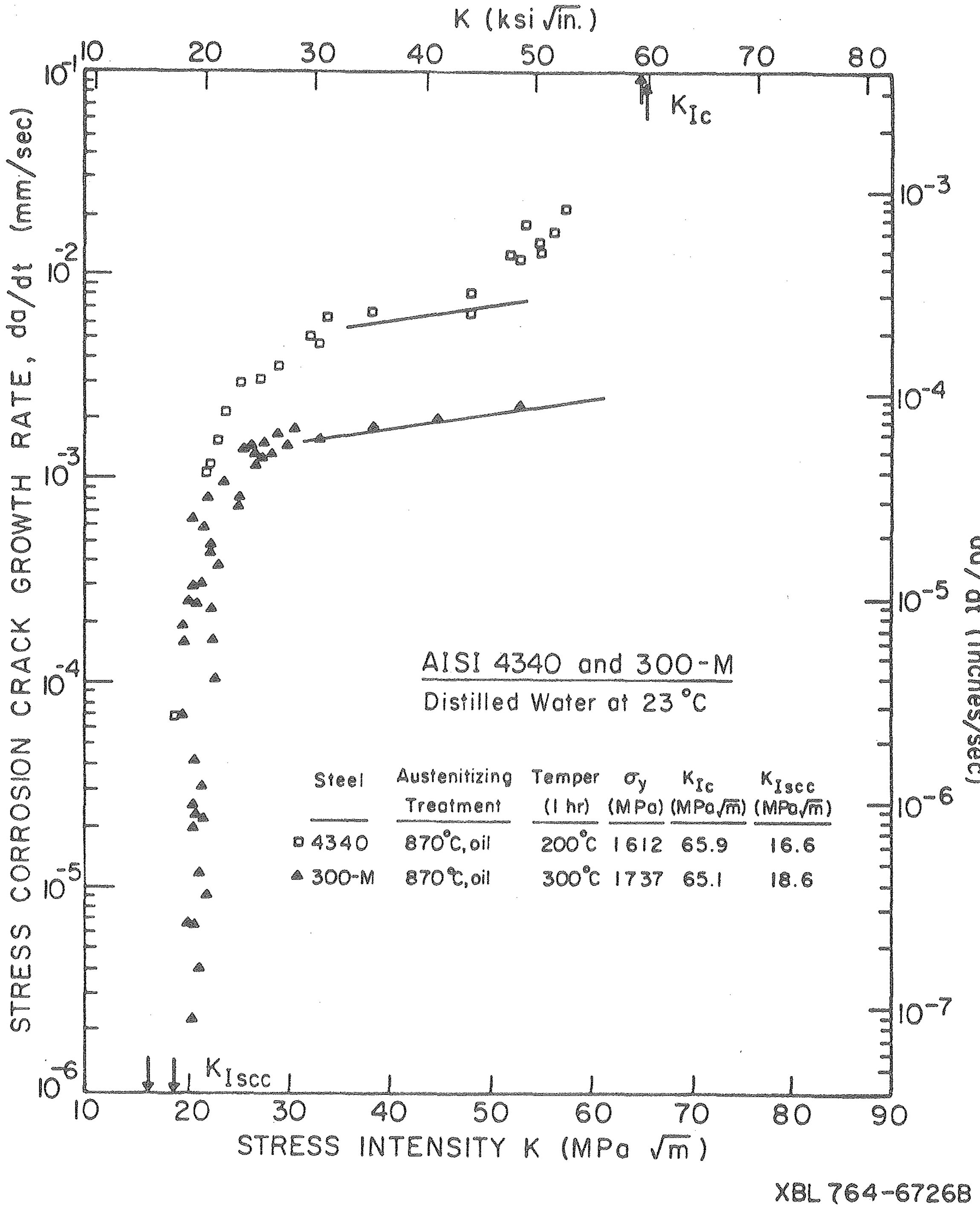
K (ksi √in.)
10 20 30 40 50 60 70 80
K_{Ic}
STRESS CORROSION CRACK GROWTH RATE, da/dt (mm/sec)
10^{-1} 10^{-2} 10^{-3} 10^{-4} 10^{-5} 10^{-6}
da/dt (inches/sec)
10^{-3} 10^{-4} 10^{-5} 10^{-6} 10^{-7}
AISI 4340 and 300-M
Distilled Water at 23 °C
Steel | Austenitizing Treatment | Temper (1 hr) | σ_y (MPa) | K_{Ic} (MPa√m) | K_{Iscc} (MPa√m)
4340 | 870°C, oil | 200°C | 1612 | 65.9 | 16.6
300-M | 870°C, oil | 300°C | 1737 | 65.1 | 18.6
K_{Iscc}
10 20 30 40 50 60 70 80 90
STRESS INTENSITY K (MPa √m)
XBL 764-6726B

Fig. 4.

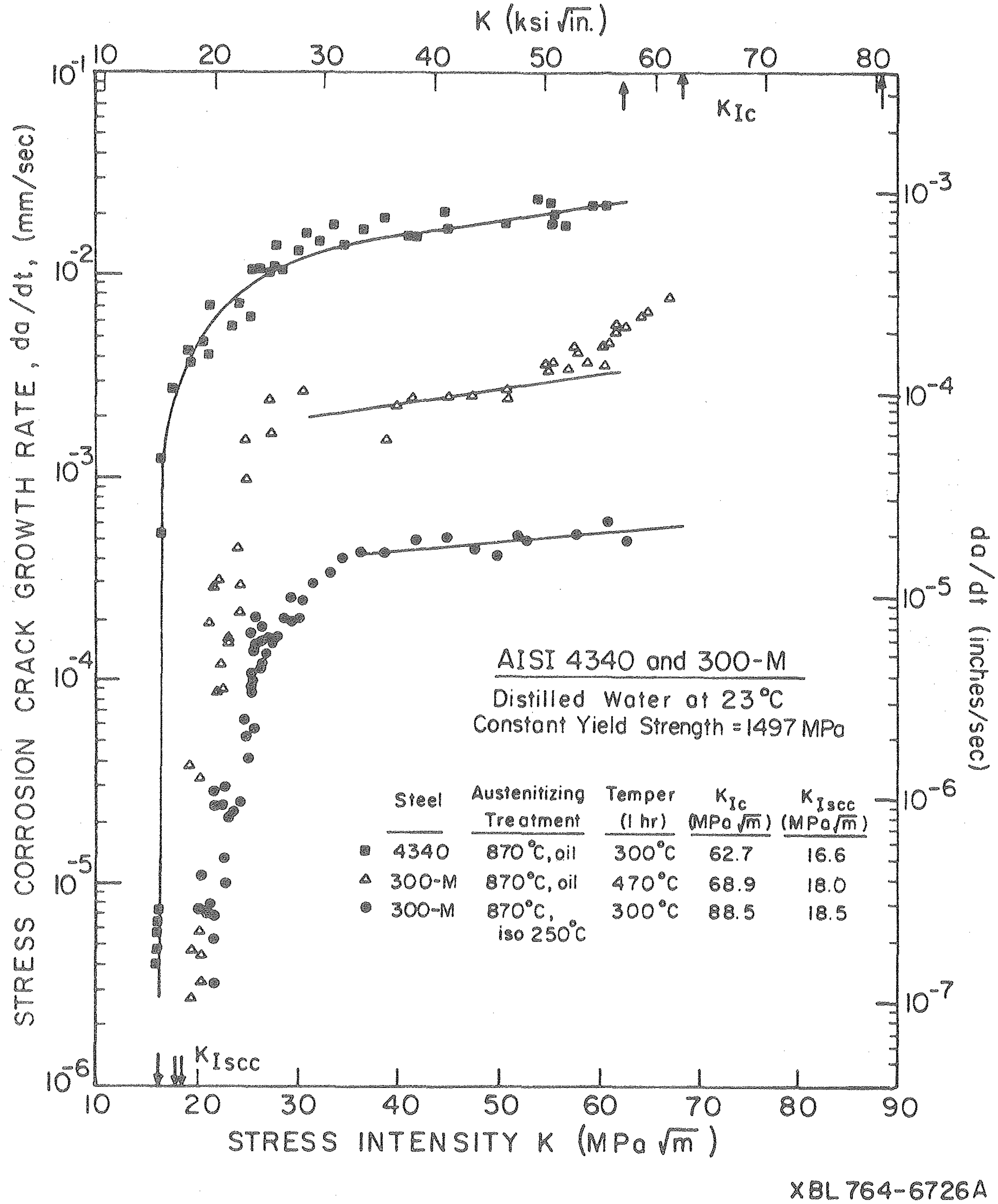
K (ksi √in.)
10
20
30
40
50
60
70
80
K_{Ic}
10^{-1}
10^{-2}
10^{-3}
10^{-4}
10^{-5}
10^{-6}
STRESS CORROSION CRACK GROWTH RATE, da/dt, (mm/sec)
10^{-3}
10^{-4}
10^{-5}
10^{-6}
10^{-7}
da/dt (inches/sec)
AISI 4340 and 300-M
Distilled Water at 23°C
Constant Yield Strength = 1497 MPa
Steel
Austenitizing Treatment
Temper (1 hr)
K_{Ic} (MPa √m)
K_{Iscc} (MPa √m)
4340
870°C, oil
300°C
62.7
16.6
300-M
870°C, oil
470°C
68.9
18.0
300-M
870°C, iso 250°C
300°C
88.5
18.5
K_{Iscc}
10
20
30
40
50
60
70
80
90
STRESS INTENSITY K (MPa √m)
XBL 764-6726A

Fig. 5.

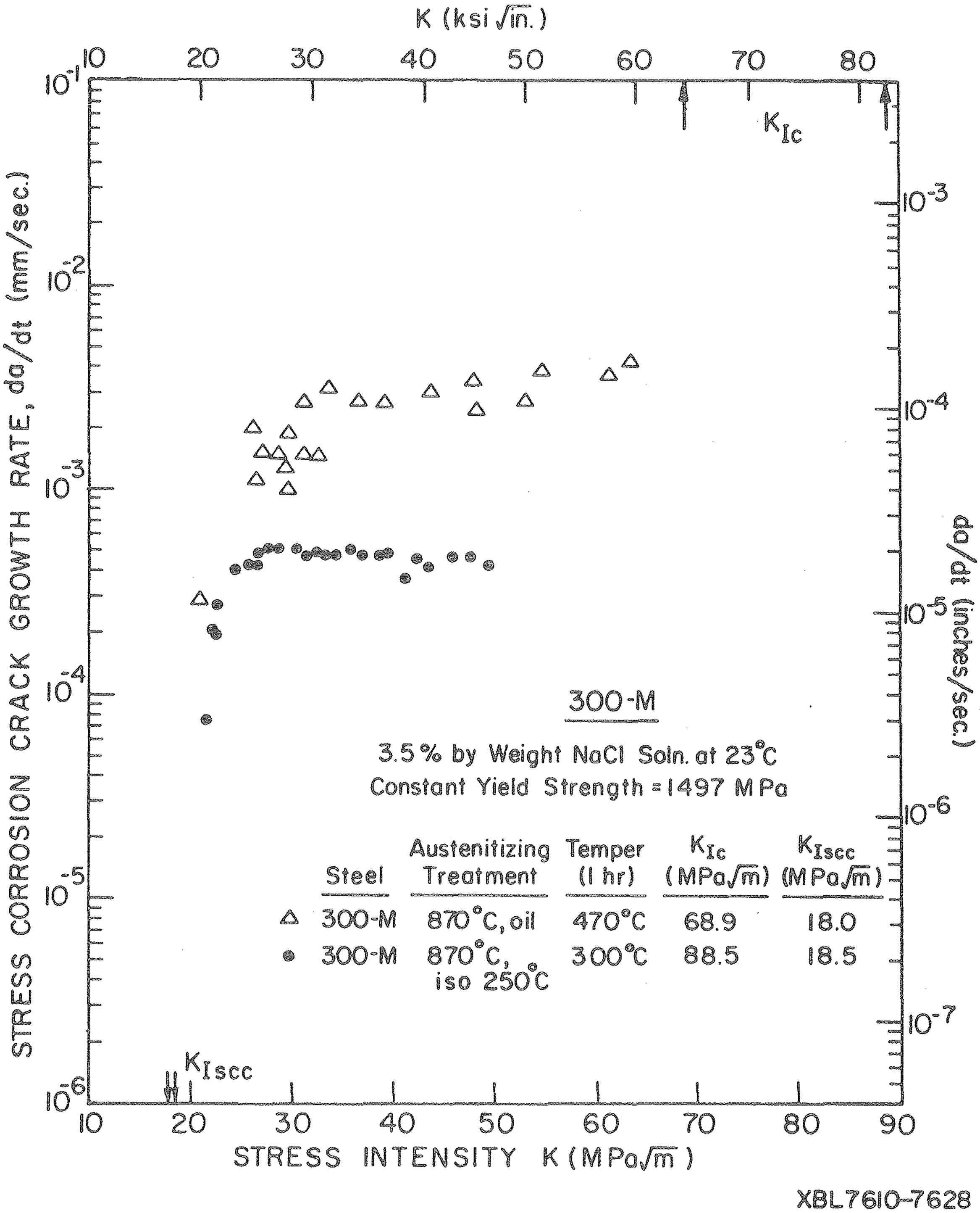
K (ksi √in.)
10
20
30
40
50
60
70
80
K_{Ic}
10^{-1}
10^{-2}
10^{-3}
10^{-4}
10^{-5}
10^{-6}
STRESS CORROSION CRACK GROWTH RATE, da/dt (mm/sec.)
10^{-3}
10^{-4}
10^{-5}
10^{-6}
10^{-7}
da/dt (inches/sec.)
300-M
3.5 % by Weight NaCl Soln. at 23°C
Constant Yield Strength = 1497 MPa
Steel
Austenitizing Treatment
Temper (1 hr)
K_{Ic} (MPa√m)
K_{Iscc} (MPa√m)
△ 300-M 870°C, oil 470°C 68.9 18.0
● 300-M 870°C, iso 250°C 300°C 88.5 18.5
K_{Iscc}
10
20
30
40
50
60
70
80
90
STRESS INTENSITY K (MPa√m)
XBL7610-7628

Fig. 6.

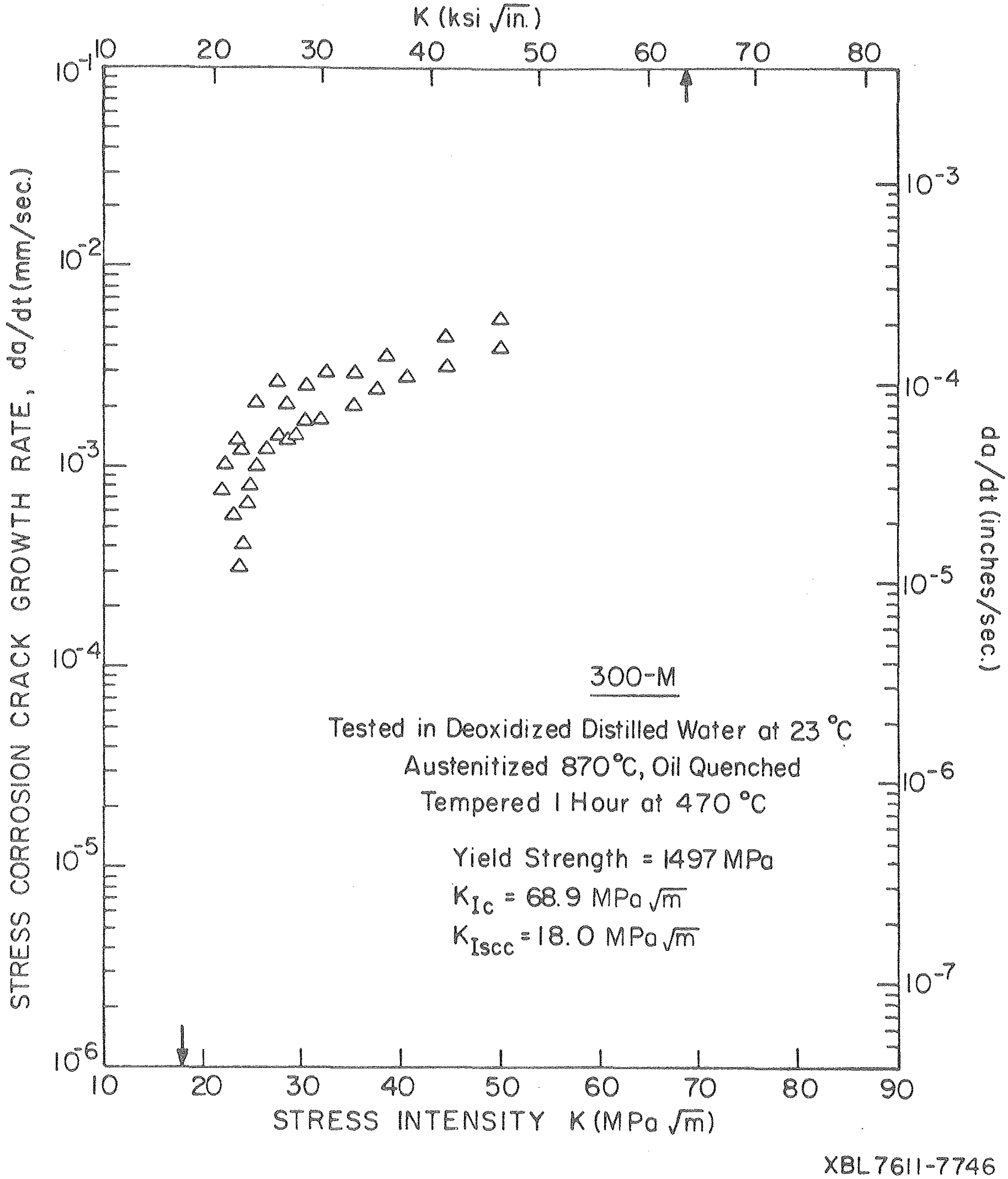
K (ksi $\sqrt{in.}$)
10
20
30
40
50
60
70
80
10^{-1}
10^{-2}
10^{-3}
10^{-4}
10^{-5}
10^{-6}
STRESS CORROSION CRACK GROWTH RATE, da/dt (mm/sec.)
10^{-3}
10^{-4}
10^{-5}
10^{-6}
10^{-7}
da/dt (inches/sec.)
300-M
Tested in Deoxidized Distilled Water at 23 °C
Austenitized 870°C, Oil Quenched
Tempered 1 Hour at 470 °C
Yield Strength = 1497 MPa
K_{Ic} = 68.9 MPa $\sqrt{m}$
K_{Iscc} = 18.0 MPa $\sqrt{m}$
10
20
30
40
50
60
70
80
90
STRESS INTENSITY K (MPa $\sqrt{m}$)
XBL 7611-7746

Fig. 7.

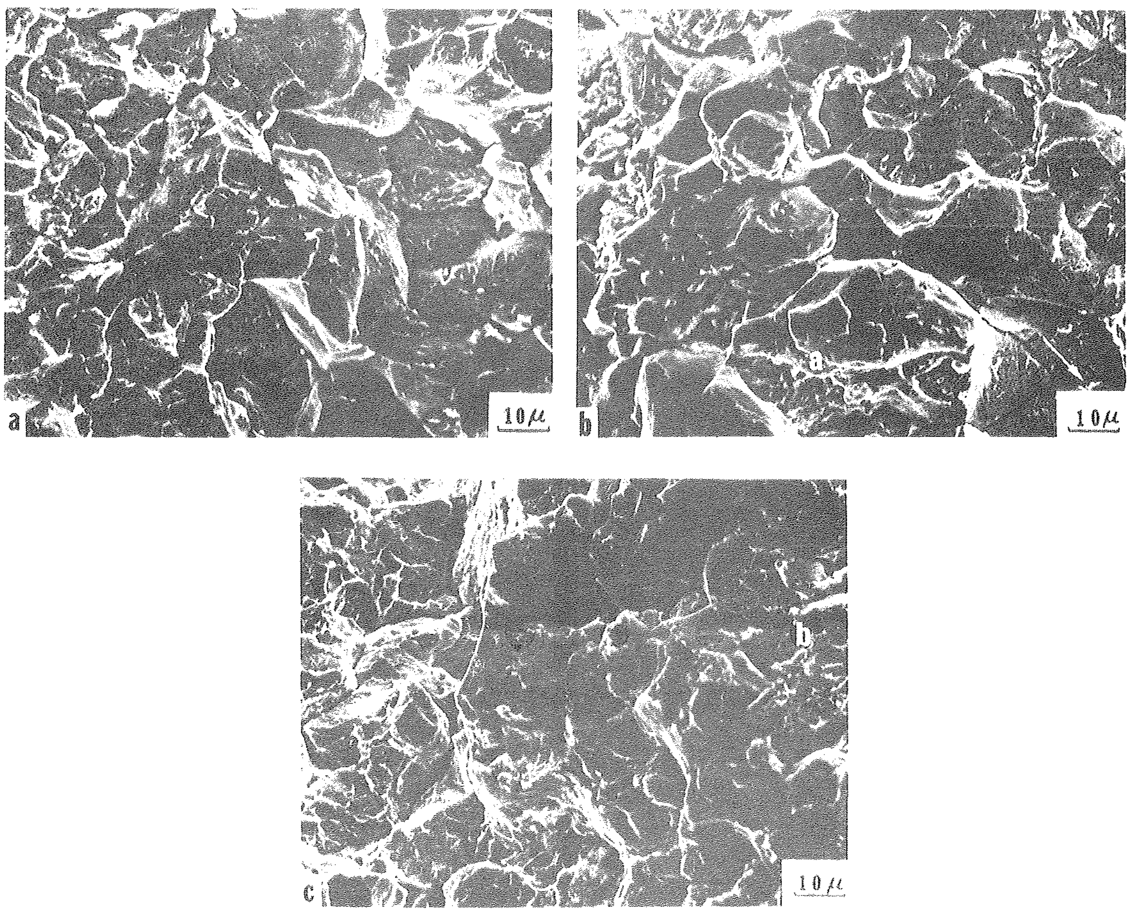

XBB 7611-10107

Fig. 8.

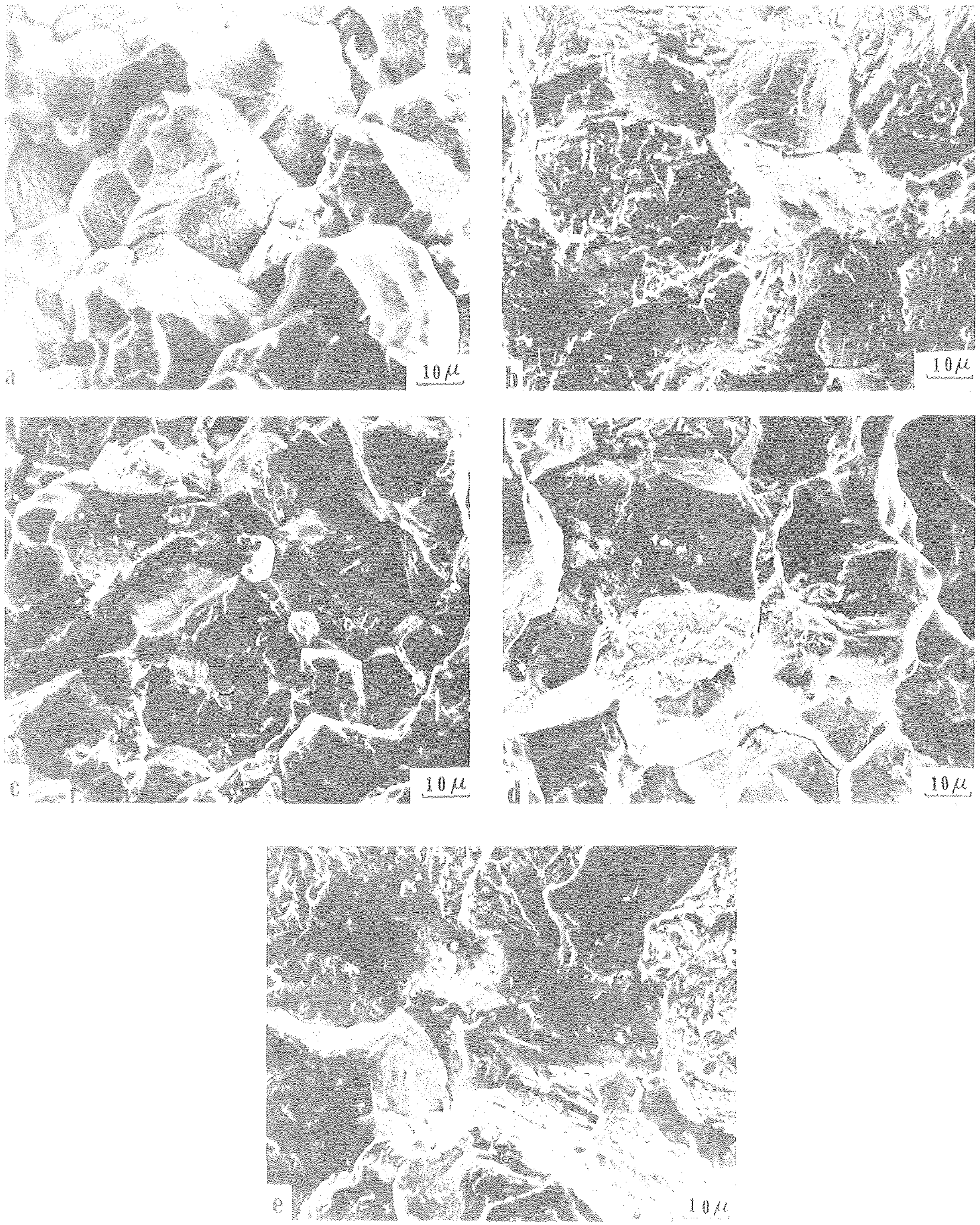

XBB 7611-10108

Fig. 9.

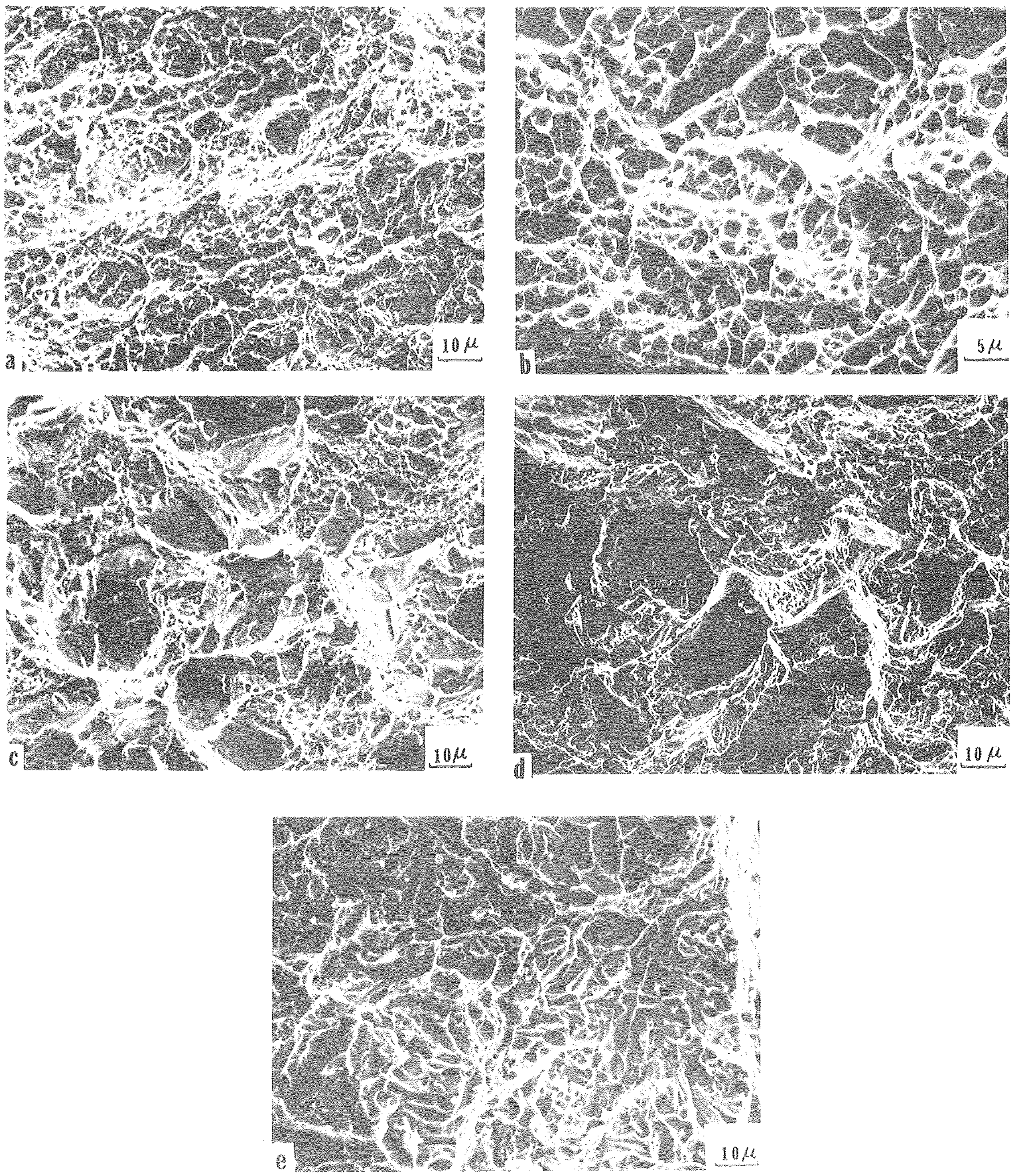

XBB 7611-10109

Fig. 10.

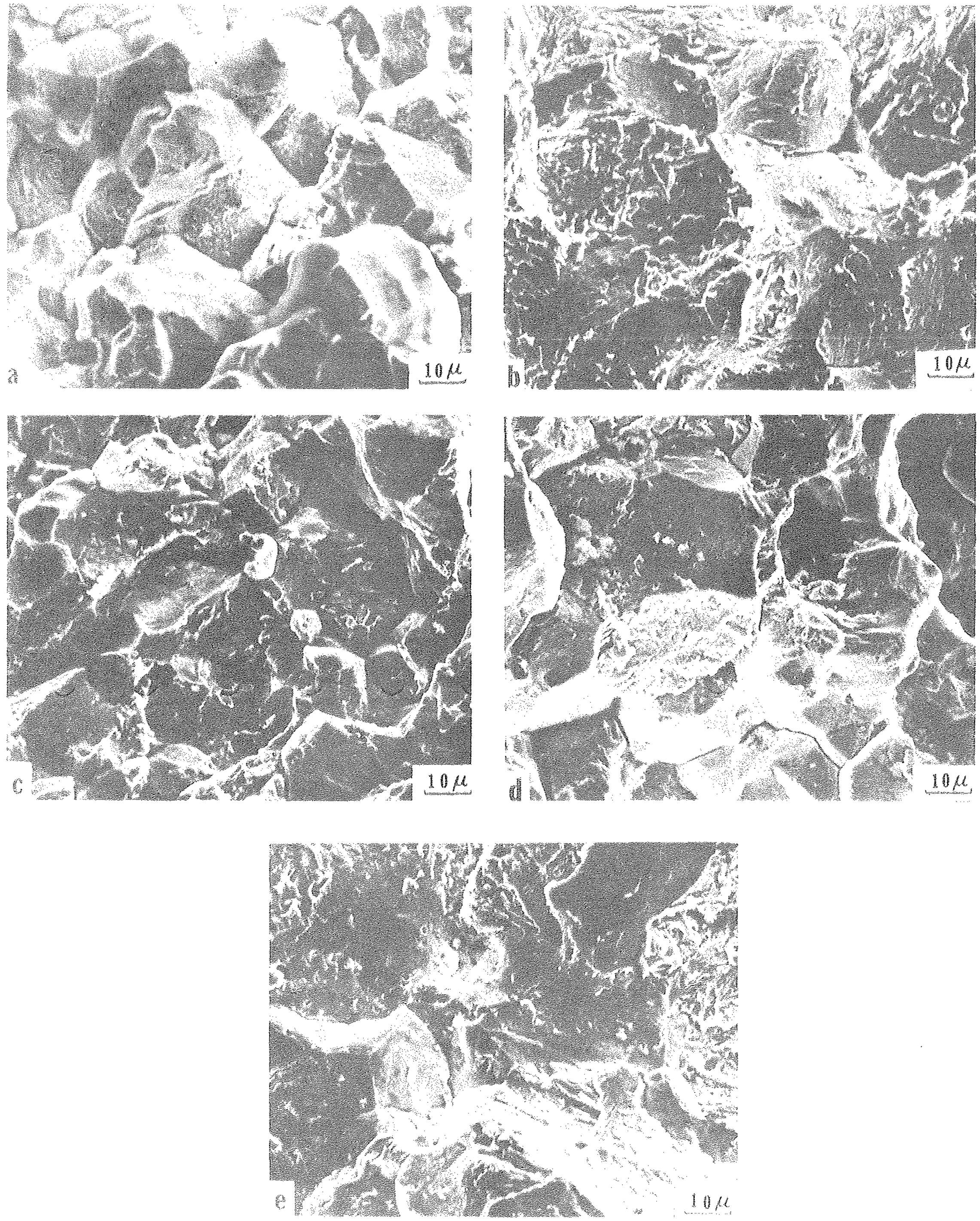

XBB 7611-10108

Fig. 9.

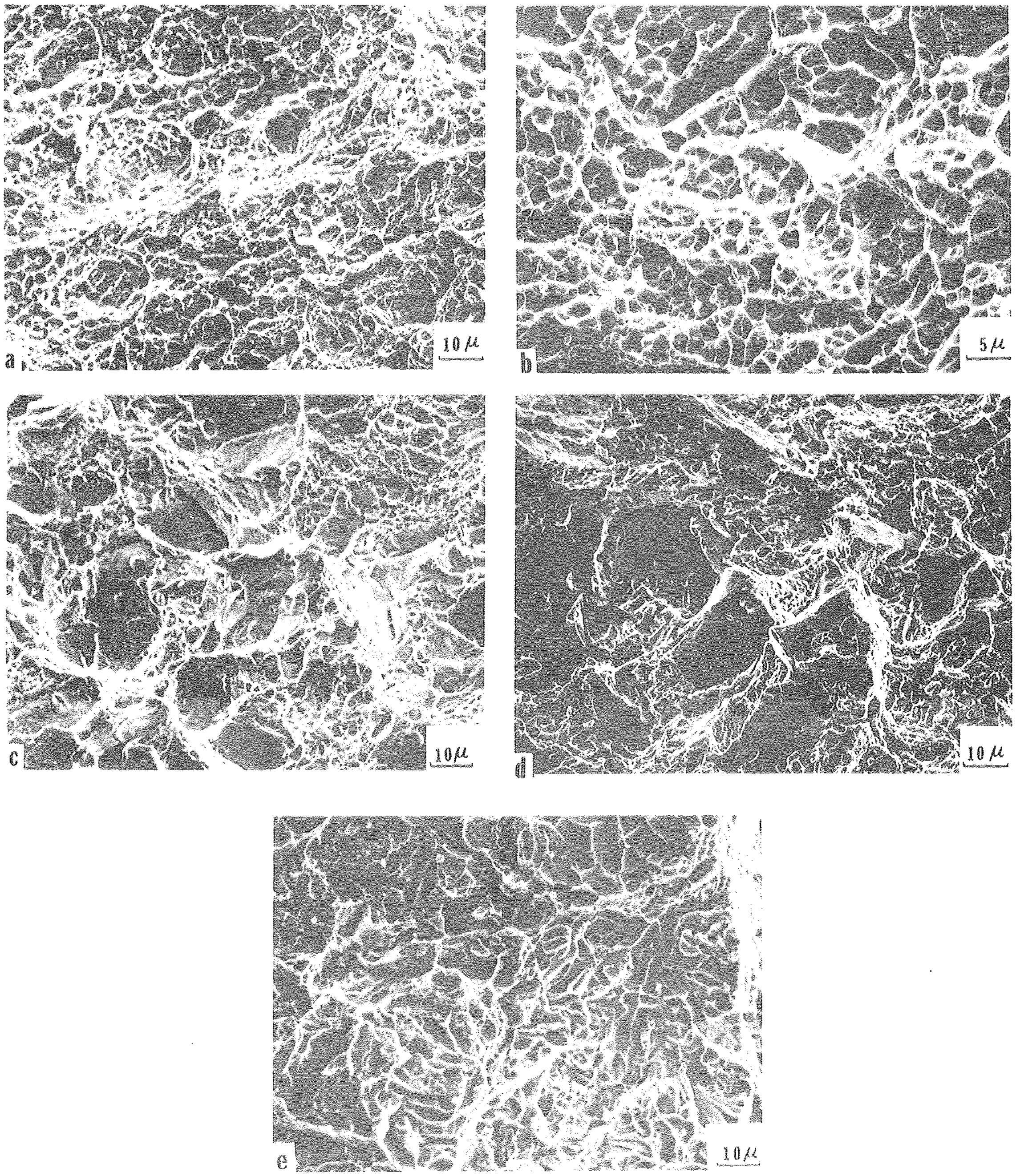

XBB 7611-10109

Fig. 10.

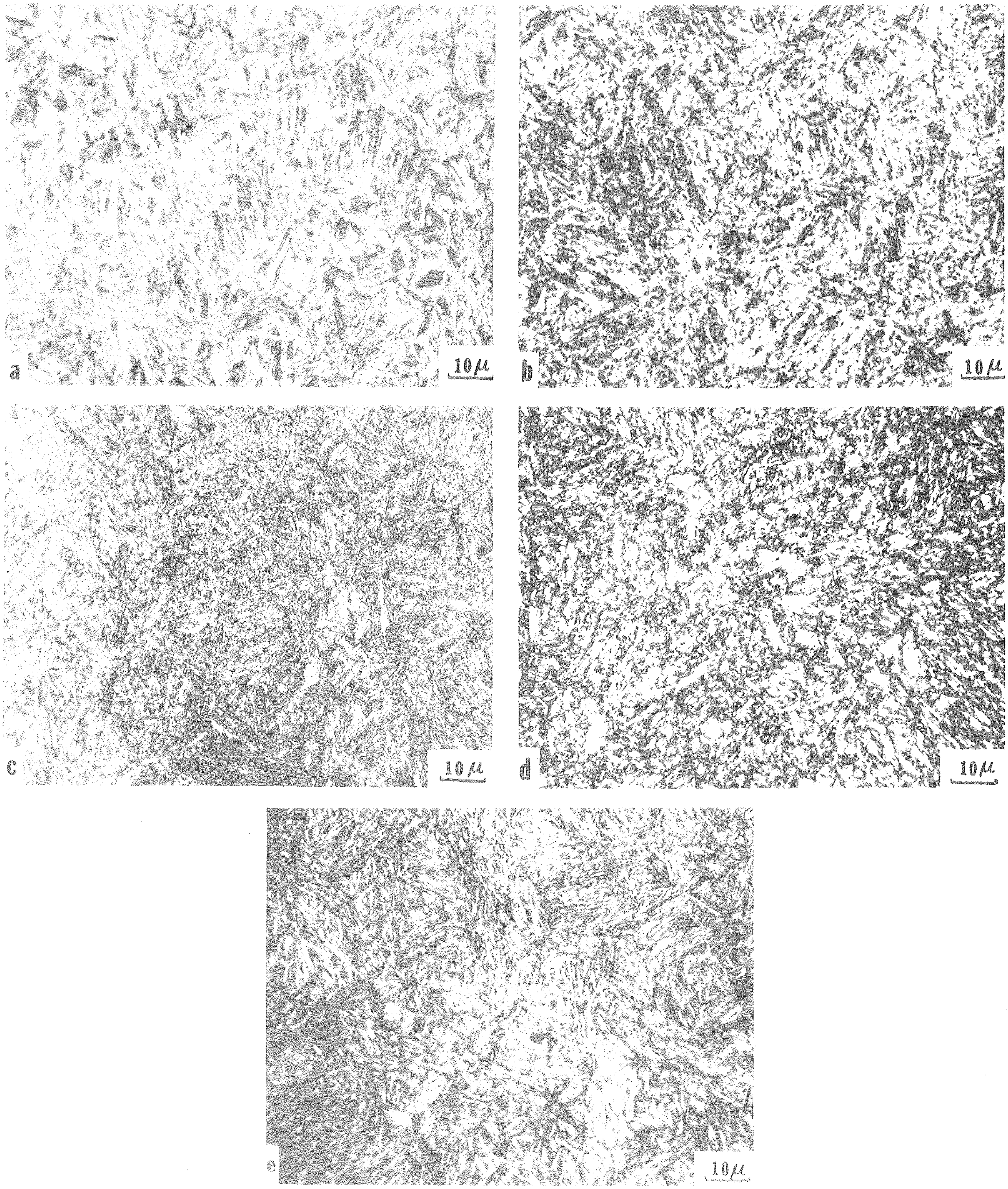

XBB 760-10802

Fig. 11.

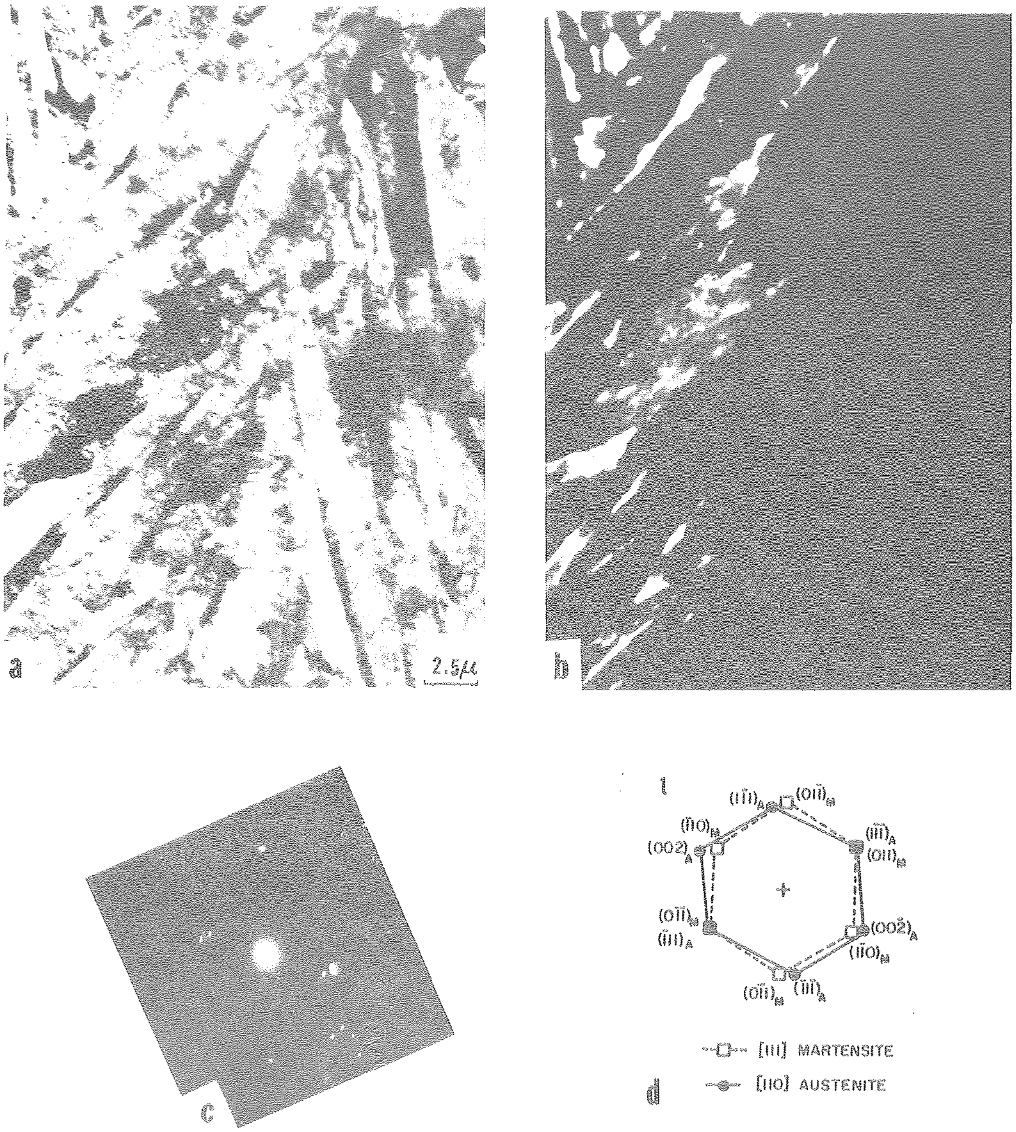

XBB 7610-9113

Fig. 12.

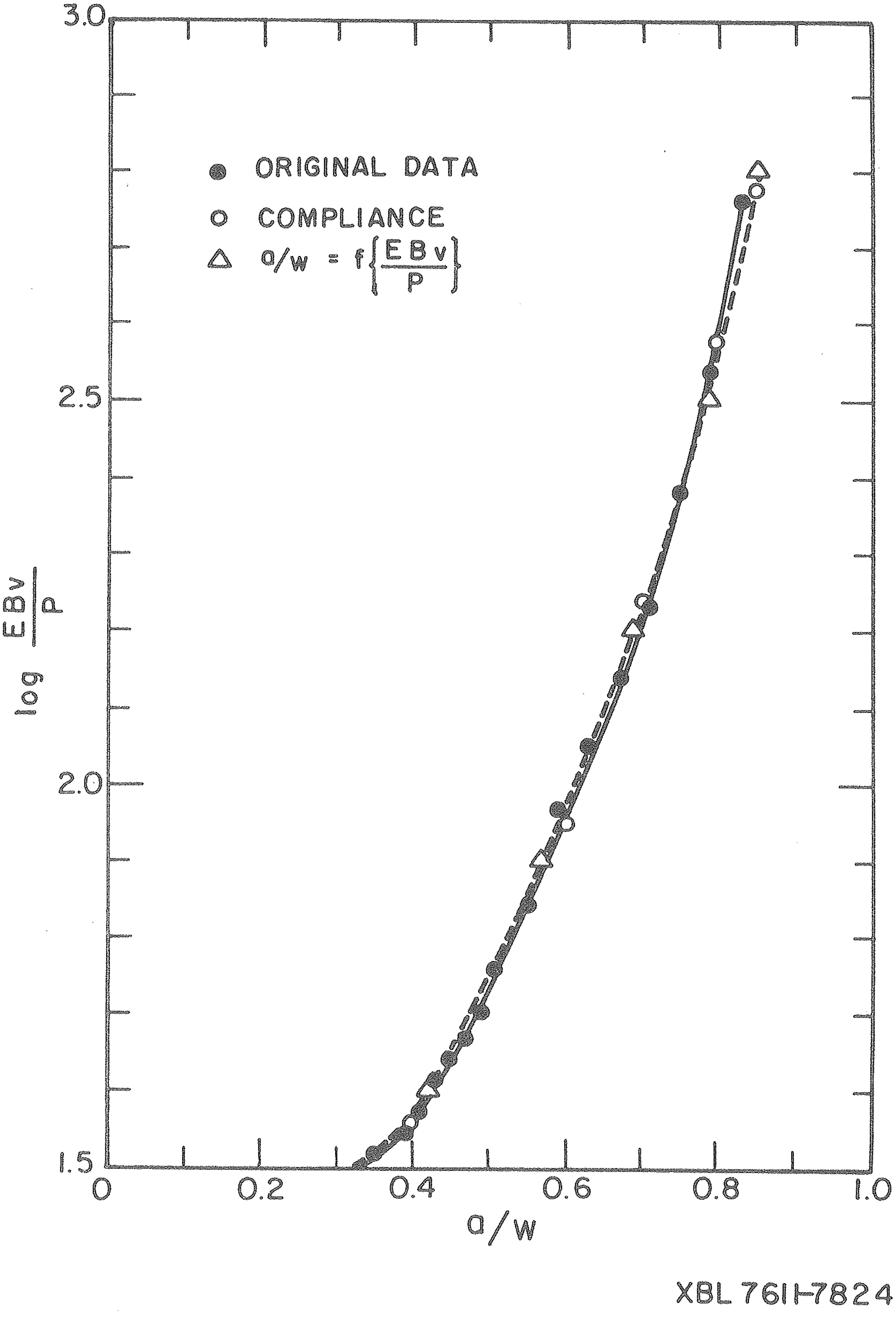
ORIGINAL DATA
COMPLIANCE
a/w = f{EBv/P}
log EBv/P
3.0
2.5
2.0
1.5
0
0.2
0.4
0.6
0.8
1.0
a/w
XBL 7611-7824

Fig. 13.

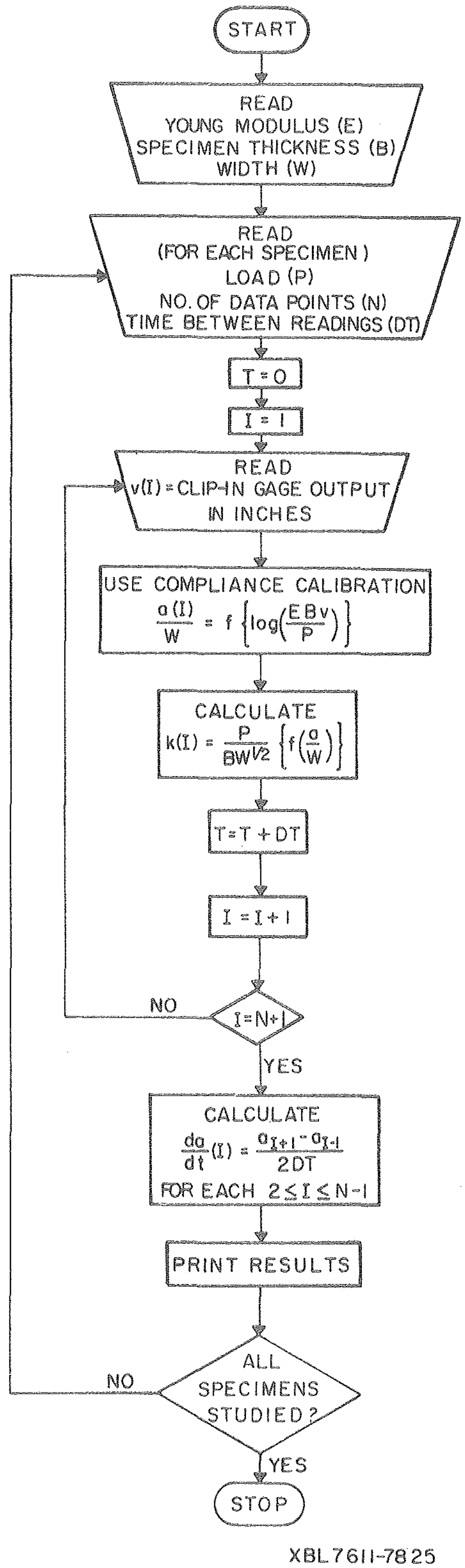
START
READ
YOUNG MODULUS (E)
SPECIMEN THICKNESS (B)
WIDTH (W)
READ
(FOR EACH SPECIMEN)
LOAD (P)
NO. OF DATA POINTS (N)
TIME BETWEEN READINGS (DT)
T = 0
I = 1
READ
v(I) = CLIP-IN GAGE OUTPUT
IN INCHES
USE COMPLIANCE CALIBRATION
$\frac{a(I)}{W} = f\left\{\log\left(\frac{EBv}{P}\right)\right\}$
CALCULATE
$k(I) = \frac{P}{BW^{1/2}}\left\{f\left(\frac{a}{W}\right)\right\}$
T = T + DT
I = I + 1
NO
I = N+1
YES
CALCULATE
$\frac{da}{dt}(I) = \frac{a_{I+1} - a_{I-1}}{2DT}$
FOR EACH $2 \leq I \leq N-1$
PRINT RESULTS
NO
ALL
SPECIMENS
STUDIED?
YES
STOP
XBL 7611-7825

Fig. 14.

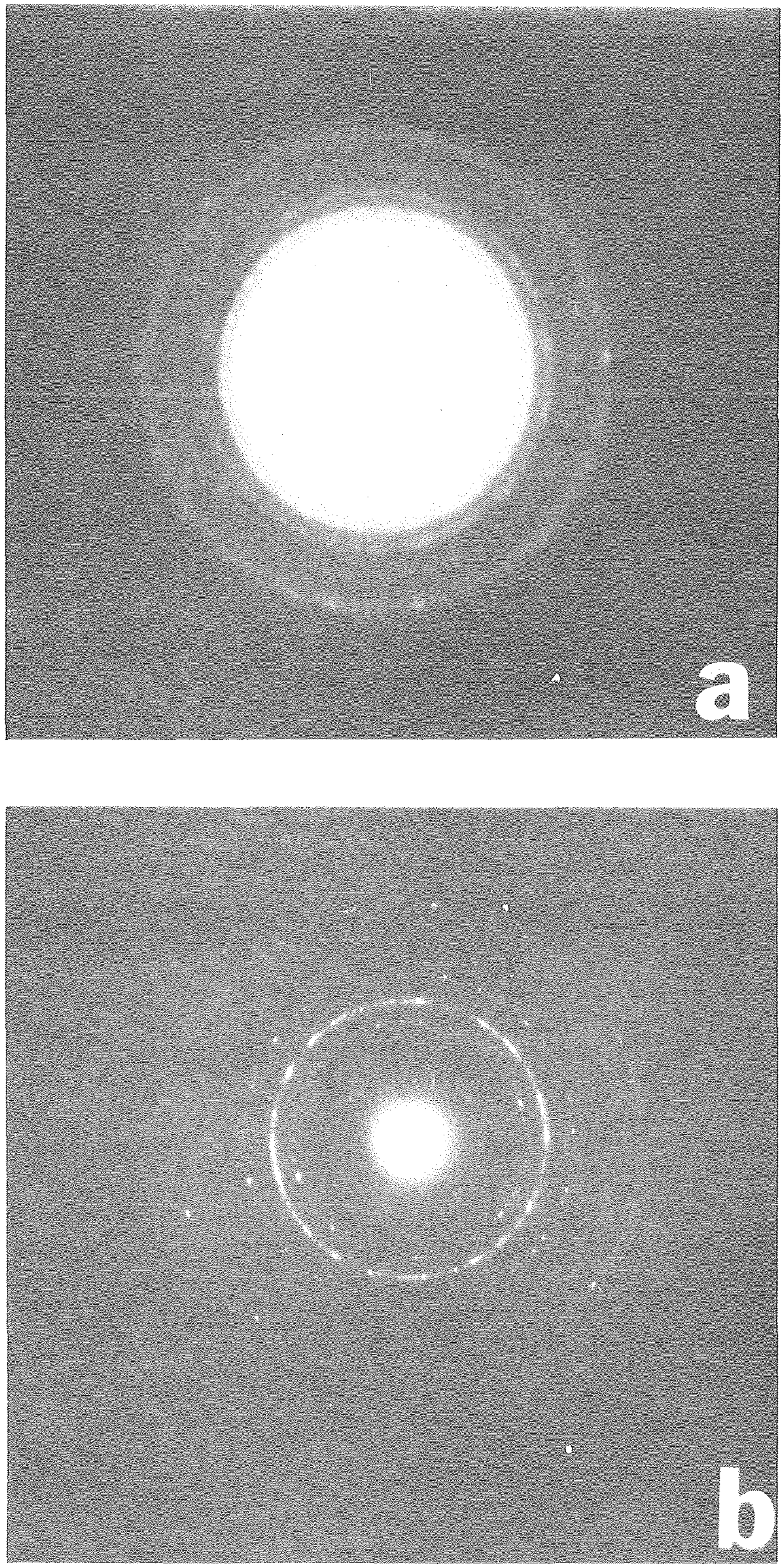

XBB 773-1686

Fig. 15.